Intracellular Mg^{2+} Enhances the Function of BK-type Ca^{2+}-activated K^+ Channels

Jingyi Shi[1,2] and Jianmin Cui[1,2]

[1]Cardiac Bioelectricity Research and Training Center, and [2]Department of Biomedical Engineering, Case Western Reserve University, Cleveland, OH 44106-7207

ABSTRACT BK channels modulate neurotransmitter release due to their activation by voltage and Ca^{2+}. Intracellular Mg^{2+} also modulates BK channels in multiple ways with opposite effects on channel function. Previous single-channel studies have shown that Mg^{2+} blocks the pore of BK channels in a voltage-dependent manner. We have confirmed this result by studying macroscopic currents of the mslo1 channel. We find that Mg^{2+} activates mslo1 BK channels independently of Ca^{2+} and voltage by preferentially binding to their open conformation. The mslo3 channel, which lacks Ca^{2+} binding sites in the tail, is not activated by Mg^{2+}. However, coexpression of the mslo1 core and mslo3 tail produces channels with Mg^{2+} sensitivity similar to mslo1 channels, indicating that Mg^{2+} sites differ from Ca^{2+} sites. We discovered that Mg^{2+} also binds to Ca^{2+} sites and competitively inhibits Ca^{2+}-dependent activation. Quantitative computation of these effects reveals that the overall effect of Mg^{2+} under physiological conditions is to enhance BK channel function.

KEY WORDS: magnesium • calcium • BK channel • ion channel gating • competitive inhibition

INTRODUCTION

Intracellular free Mg^{2+} concentration has been measured to be between 0.4 and 3 mM under normal physiological conditions (Flatman, 1984; Gupta et al., 1984; Corkey et al., 1986; Flatman, 1991). At such concentrations, Mg^{2+} modulates a variety of Ca^{2+} and K^+ channels to affect the excitability or excitation-contraction coupling in neurons, cardiac myocytes, and smooth muscle cells (Altura et al., 1987; Matsuda et al., 1987; Vandenberg, 1987; White and Hartzell, 1988; Altura and Gupta, 1992; Chuang et al., 1997; Romani et al., 2000). After central nervous system injury, $[Mg^{2+}]_i$ is significantly reduced, contributing to a number of factors including increased neurotransmitter release and oxidative stress that initiate an autodestructive cascade of biochemical and pathophysiological changes, known as secondary injury, that ultimately results in irreversible tissue damage (Vink and Cernak, 2000). Pharmacological studies have shown that Mg^{2+} may be an effective therapeutic agent after neurotrauma to improve survival and motor outcome and to alleviate cognitive deficits (Vink and Cernak, 2000). Magnesium supplements are also important in the prevention and management of cardiovascular diseases that predispose to hypertension or congestive heart failure (Laurant and Touyz, 2000; Seelig, 2000).

The activation of large conductance Ca^{2+} activated K^+ channels (BK channels)* depends on both voltage and intracellular calcium (Marty, 1981; Pallotta et al., 1981). Because of this property, BK channels are uniquely suited to play a role in biological processes that involve both calcium signaling and voltage changes. These include neurotransmitter release (Robitaille et al., 1993; Yazejian et al., 1997), electric tuning of cochlear hair cells (Hudspeth and Lewis, 1988a,b; Wu et al., 1995), and vascular smooth muscle contraction (Nelson et al., 1995; Brenner et al., 2000; Pluger et al., 2000). The function of BK channels is further modulated by intracellular Mg^{2+}, resulting in a reduced single-channel conductance (Ferguson, 1991; Zhang et al., 1995; Morales et al., 1996; Wachter and Turnheim, 1996), an increased open probability at certain $[Ca^{2+}]_i$ (Squire and Petersen, 1987; Zamoyski et al., 1989; McLarnon and Sawyer, 1993; Zhang et al., 1995; Bringmann et al., 1997), and an increased apparent cooperativity of Ca^{2+} in activating the channel (Golowasch et al., 1986; Oberhauser et al., 1988; Trieschmann and Isenberg, 1989). These Mg^{2+} effects on BK channel function may contribute significantly to its physiological and pathophysiological roles.

A series of previous studies have focused on the Mg^{2+} block of BK channels. These studies have suggested that Mg^{2+} reduces the single-channel conductance by binding to a site inside the pore with fast kinetics and blocking the channel (Ferguson, 1991; Laver, 1992;

Address correspondence to Dr. Jianmin Cui, Department of Biomedical Engineering, Case Western Reserve University, Cleveland, OH 44106-7207. Fax: (216) 368-4969; E-mail: jxc93@cwru.edu

*Abbreviations used in this paper: BK channels, Ca^{2+}-activated K^+ channels; MWC, Monod-Wyman-Changeux; P_o, open probability.

Zhang et al., 1995; Morales et al., 1996). However, the mechanism by which Mg^{2+} increases the channel open probability and the cooperativity of Ca^{2+}-dependent activation is not clear. In particular, how voltage, Ca^{2+}, and Mg^{2+} interact during channel activation is not elucidated. The increased cooperativity of Ca^{2+}-dependent activation by Mg^{2+} was taken to suggest that Mg^{2+} exposed Ca^{2+} binding sites that had been buried in BK channels before Mg^{2+} was added, bringing the total Ca^{2+} binding sites to be more than six (Golowasch et al., 1986). However, the extent to which Mg^{2+} affects BK channel activation seemed to depend on $[Ca^{2+}]_i$. At certain $[Ca^{2+}]_i$ Mg^{2+} activated the channel, whereas at other $[Ca^{2+}]_i$ Mg^{2+} had little effect or even reduced channel activation (Zhang et al., 1995; Komatsu et al., 1996; Kazachenko and Chemeris, 1998). These results have not been explained with a single molecular mechanism. Such lack of understanding in the molecular mechanism combined with the complexity derived from the opposing Mg^{2+} actions of channel block and channel activation make it difficult to assess the physiological consequence of Mg^{2+} effects on BK channels.

Recent studies on cloned *slo* family of BK channels have revealed that voltage and Ca^{2+} activate BK channels through distinct mechanisms (Cox et al., 1997a; Cui et al., 1997; Horrigan et al., 1999; Cui and Aldrich, 2000). Similar to voltage-gated K^+ channels, BK channels contain the S4 domain that may function as an intrinsic voltage sensor (Atkinson et al., 1991; Adelman et al., 1992; Butler et al., 1993; Aggarwal and MacKinnon, 1996; Mannuzzu et al., 1996; Seoh et al., 1996; Diaz et al., 1998; Cui and Aldrich, 2000). In response to membrane depolarization, BK channels can be activated in the absence of Ca^{2+} binding (Pallotta, 1985; Meera et al., 1996; Cui et al., 1997; Horrigan et al., 1999). Ca^{2+} binds to the channel at sites located in the intracellular carboxyl terminus of the α subunit (Moss et al., 1996; Schreiber et al., 1999; Bian et al., 2001) with a high affinity (K_d = ~1–10 μM; McManus and Magleby, 1991; Cox et al., 1997a). It modulates the responses of the channel to voltage by shifting the voltage dependence of the steady-state open probability (P_o) and the activation kinetics to a more negative voltage range (Marty, 1981; Pallotta et al., 1981; McManus and Magleby, 1991; Adelman et al., 1992; Cox et al., 1997a; Cui et al., 1997). Both voltage- and Ca^{2+}-dependent activation of the channel involve allosteric mechanisms (Cox et al., 1997a; Cui et al., 1997; Horrigan et al., 1999) that are individually well described by Monod-Wyman-Changeux (MWC; Monod et al., 1965)–type models for allosteric proteins (McManus and Magleby, 1991; Cox et al., 1997a; Horrigan and Aldrich, 1999; Horrigan et al., 1999). It has been demonstrated that although voltage sensor movements and Ca^{2+} binding both activate the channel, they do not affect each other directly. The voltage- and Ca^{2+}-dependent mechanism activate the channel through separate pathways, and then converge to affect the final transition between the open and closed conformation (Cui and Aldrich, 2000). In this study, we investigate whether Mg^{2+} activates the channel by affecting the separate voltage or Ca^{2+}-dependent activation, or by affecting the final transition between the open and closed conformation. Our results demonstrate that Mg^{2+}-dependent activation does not directly depend on voltage or Ca^{2+} but the binding of Mg^{2+} will affect the close-open transition. We have also discovered that in addition to activation of the channel, Mg^{2+} also binds to the high affinity Ca^{2+} sites and competitively inhibits Ca^{2+}-dependent activation. The combination of Mg^{2+}-dependent activation and competitive inhibition increases the apparent cooperativity of the response of mslo1 to Ca^{2+}. The quantitative description of each individual Mg^{2+} effect enabled us to estimate the overall effect of intracellular Mg^{2+} on BK channel function under physiological conditions.

An abstract of this work has been presented in the 45th Annual Meeting of Biophysical Society.

MATERIALS AND METHODS

Clones and Channel Expression

The mbr5 clone of mslo1 (Butler et al., 1993), the cDNA of mslo3 (Schreiber et al., 1998), and mslo3 tail (Schreiber et al., 1999) were provided to us by Dr. Larry Salkoff (Washington University School of Medicine, St. Louis, MO). The cDNA of mslo1 core, including nucleotides 1–2,025 of the coding region (Met 1–Lys 648) subcloned into PSD64TF, was provided to us by Dr. Yasushi Okamura (National Institute of Advanced Industrial Science and Technology, Tsukuba, Japan). cRNA was transcribed in vitro using the "mMessage mMachine" kit with T3 or SP6 polymerase (Ambion Inc.). 0.05–0.5 ng of cRNA were injected into *Xenopus laevis* oocytes 2–6 d before recording.

Electrophysiology

Macroscopic currents were recorded from inside-out patches formed with borosilicate pipettes of 1~2 megohm resistance. Data were acquired using an Axopatch 200-B patch-clamp amplifier (Axon Instruments, Inc.) and Pulse acquisition software (HEKA Electronik). Records were digitized at 20-μs intervals and low-pass filtered at 10 kHz with the 4-pole Bessel filter (Axon Instruments, Inc.). The pipette solution contained the following (in mM): 140 potassium methanesulfonic acid, 20 HEPES, 2 KCl, and 2 $MgCl_2$, pH 7.20. The basal internal solution contained the following (in mM): 140 potassium methanesulfonic acid, 20 HEPES, 2 KCl, and 1 EGTA, pH 7.20. Methanesulfonic acid was purchased from Sigma-Aldrich. The "0 $[Ca^{2+}]_i$" solution was the same as the basal internal solution except that it contained 5 mM EGTA, having a free $[Ca^{2+}]_i$ of ~0.5 nM that was too low to affect mslo1 channel activation (Cui et al., 1997). $MgCl_2$ was added to these internal solutions to give the appropriate free $[Mg^{2+}]_i$. $CaCl_2$ was added to the basal internal solutions with amounts calculated using a program similar to published (Fabiato and Fabiato, 1979) to give rise various free $[Ca^{2+}]_i$. The free $[Ca^{2+}]_i$ was then measured with a calcium-sensitive electrode (Orion Research Inc.) with the same procedure as previously described (Cox et al., 1997b). Al-

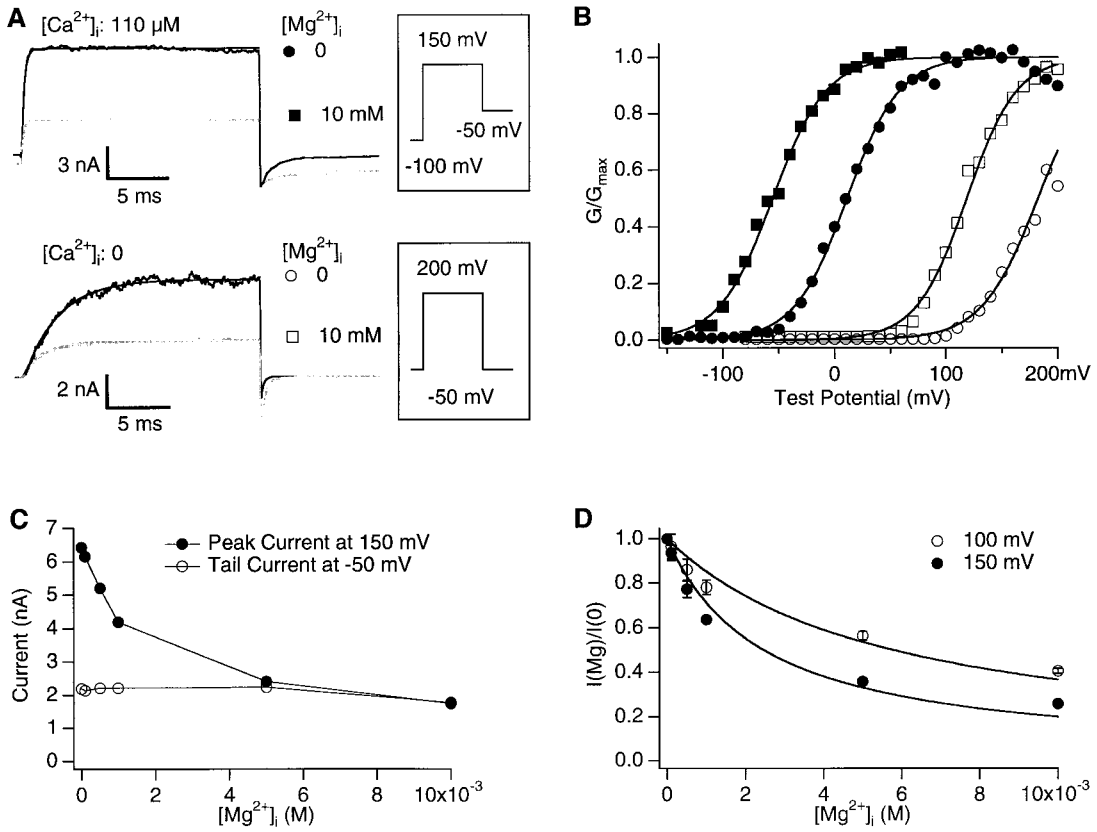

FIGURE 1. Intracellular Mg^{2+} blocks and activates mslo1 channels. (A) mslo1 currents recorded from an inside-out patch with 0 (dark traces) or 10 mM (light traces) $[Mg^{2+}]_i$ at $[Ca^{2+}]_i$ of 0 (bottom) and 110 μM (top). The voltage protocols are schematically displayed next to the current traces. At 110 μM $[Ca^{2+}]_i$, the holding, test, and repolarizing potentials were −100, 150, and −50 mV, respectively. At 0 $[Ca^{2+}]_i$, they were −50, 200, and −50 mV, respectively. Smooth lines are exponential fits to current traces. The time constant is 0.23 ms at 0 $[Mg^{2+}]_i$, 0.26 ms at 10 mM $[Mg^{2+}]_i$ with 110 μM $[Ca^{2+}]_i$ and 2.84 ms at 0 $[Mg^{2+}]_i$, 1.72 ms at 10 mM $[Mg^{2+}]_i$ with 0 $[Ca^{2+}]_i$. (B) G-V relations of mslo1 channels with 0 (circles) or 10 mM (squares) $[Mg^{2+}]_i$ at $[Ca^{2+}]_i$ of 0 (open symbols) and 110 μM (closed symbols). Corresponding symbols are also shown in A. The smooth lines are fits with the Boltzmann function, $G/G_{max} = 1/(1 + \exp(-ze(V - V_{1/2})/kT))$, where G is conductance, z is the valence of equivalent charge, e is the elementary charge, $V_{1/2}$ is the voltage where conductance is half-maximum, k is Boltzmann's constant, and T is the absolute temperature. At 110 μM $[Ca^{2+}]_i$, z = 1.08 and $V_{1/2}$ = 11.4 mV with 0 $[Mg^{2+}]_i$, and z = 0.92, $V_{1/2}$ = −52.4 mV with 10 mM $[Mg^{2+}]_i$. At 0 $[Ca^{2+}]_i$, z = 1.01 and $V_{1/2}$ = 182.6 mV with 0 $[Mg^{2+}]_i$, and z = 1.20, $V_{1/2}$ = 117.0 mV with 10 mM $[Mg^{2+}]_i$. (C) The response to $[Mg^{2+}]_i$ of the peak current at the test potential of 150 mV and the instantaneous tail current at the repolarizing potential of −50 mV. $[Ca^{2+}]_i$ was 1 μM. Data points are connected by thin straight lines. (D) Mg^{2+} block of the peak current at test potentials of 100 and 150 mV. The ratio of the current with internal Mg^{2+} to that without internal Mg^{2+}, I(Mg)/I(0), from three (at 150 mV) or five (at 100 mV) patches were averaged and plotted versus $[Mg^{2+}]_i$. Error bars in all figures represent the SEM. Smooth lines are fits of the Woodhull model (Woodhull, 1973) $I(Mg)/I(0) = 1/(1 + [Mg^{2+}]_i / K_D(0)\exp(-2\delta eV/kT))$, where $K_D(0)$ = 31.5 mM is the dissociation constant at 0 mV and δ = 0.22 is the fraction of the voltage across the membrane that influences Mg^{2+} at its binding site, as measured from the intracellular surface.

though theoretically only $[Ca^{2+}]_i \geq 10$ μM can be accurately measured by the calcium-sensitive electrode, we find that the response of the electrode (mV) to $\log([Ca^{2+}]_i)$ between ~1 and 10 μM by calculation follows well the same straight line as at $[Ca^{2+}]_i \geq 10$ μM. The calcium-sensitive electrode was always calibrated right before measurements, and then recalibrated immediately after measurements. The results of calibration and recalibration were the same, indicating that the electrode was stable during measurements. The presence of Mg^{2+} in the solution had negligible effects on the accuracy of such measurements. The response of mslo1 channels was also compared with previous results to ensure that each time the $[Ca^{2+}]_i$ was measured correctly. Since the activity of mslo3 channels is pH-dependent (Schreiber et al., 1998) in the recording of mslo3 channels, the pH of internal solutions was adjusted to be 8.0. Mg^{2+} effects on mslo1 channels were not affected by pH. A sewer pipe flow system (model DAD12; Adams and List Assoc. Ltd.) was used to supply and exchange the internal solution to the cytoplasmic face of the patch. Experiments were conducted at room temperature (23°C).

RESULTS

Separating the Activation and Block of mslo1 Channels by Intracellular Mg^{2+}

Fig. 1 shows that intracellular Mg^{2+} both reduces the current amplitude at positive voltages and shifts the conductance-voltage (G-V) relations of the mslo1 channel. In Fig. 1 A mslo1 currents were recorded from an inside-out patch with a symmetric 140 mM intra- and extracellular $[K^+]$ at 110 μM and 0 $[Ca^{2+}]_i$. At positive

voltages, 10 mM $[Mg^{2+}]_i$ reduces the outward current at both $[Ca^{2+}]_i$'s. Fig. 1 B shows the G-V relations of the mslo1 channel in the absence or presence of 10 mM $[Mg^{2+}]_i$ at 0 and 110 μM $[Ca^{2+}]_i$, respectively. At both $[Ca^{2+}]_i$'s, the G-V relation is shifted to the left on the voltage axis by ~65 mV. Thus, at any given voltages within the range of G-V relations, the mslo1 channel is activated more in the presence of 10 mM $[Mg^{2+}]_i$.

Previous single-channel studies have demonstrated a fast voltage-dependent block of BK channels by intracellular Mg^{2+}, resulting in a reduction of single-channel conductance at positive voltages (Ferguson, 1991; Laver, 1992). Our results indicate that the same block causes the reduction of the current amplitude at the macroscopic current level. First, the Mg^{2+} block is voltage-dependent: 10 mM $[Mg^{2+}]_i$ blocks the outward current at 150 mV, but the instantaneous tail current at the repolarizing potential of −50 mV is similar in size with or without Mg^{2+} (Fig. 1 A, 110 μM $[Ca^{2+}]_i$). In both cases, the mslo1 channel is fully activated at 150 mV and 110 μM $[Ca^{2+}]_i$ (Fig. 1 B) so that the similar instantaneous tail current indicates that the single-channel conductance is the same at the repolarizing potential of −50 mV with or without Mg^{2+}. Thus, the negative voltage of −50 mV relieves the Mg^{2+} block of the channel at the preceding 150 mV. Similarly shown in Fig. 1 C, the block of the peak current at 150 mV increases with increasing $[Mg^{2+}]_i$, whereas the instantaneous tail current at −50 mV is not blocked and remains the same for the entire range of $[Mg^{2+}]_i$. Fig. 1 D plots the averaged dose–response of the block at 100 and 150 mV, showing that Mg^{2+} induced block is more pronounced at higher voltages. The curves are fit by the Woodhull model (Woodhull, 1973; Fig. 1 D, legend) with K_D of 31.5 mM at 0 mV and electric distance of 0.22 from the inside of the membrane. These results are similar to those obtained previously from studies at the single-channel level (Ferguson, 1991; Laver, 1992). Second, the relief of the Mg^{2+} block is very fast, at least faster than the time resolution of our macroscopic current recording (≪0.1 ms) so that all the blockade has been relieved at the beginning of tail current measurements. Similarly, the block at positive voltages is also fast. The activation time course of mslo1 channels can be fit with a single-exponential function in the absence as well as in the presence of intracellular Mg^{2+} with similar time constants (Fig. 1 A; Cui et al., 1997; Horrigan et al., 1999). Therefore, the time course of Mg^{2+} block is much faster than the time course of channel activation at 150 mV and 110 μM $[Ca^{2+}]_i$ (~0.25 ms, Fig. 1 A).

The characteristics of the Mg^{2+} block allowed us to construct G-V relations by measuring the tail current amplitude at a fixed negative voltage of −50 mV after each test potential (Fig. 1) and separate the gating properties from the block. The tail current at −50 mV is not affected significantly by the Mg^{2+} block at $[Mg^{2+}]_i$ up to 10 mM (Fig. 1, A and C). At higher $[Mg^{2+}]_i$ such as 100 mM, a fraction of the tail current would be blocked even at −50 mV (unpublished data). However, since the block and unblock were very fast the single-channel conductance at the repolarization to −50 mV after each test pulse would reach the same value instantly. Therefore, the macroscopic tail current only reflected the differences in the amount of open channels at the end of different test pulses and G-V relations would still represent the gating properties only. A fast block of mslo1 channels by intracellular Ca^{2+} similar to the Mg^{2+} block was shown previously to be separable from the gating properties with the same treatment (Cox et al., 1997b).

Mg^{2+} Affects Gating and Permeation through Distinct Binding Sites

In the experiment shown in Fig. 1 A, at 110 μM $[Ca^{2+}]_i$, the holding potential was −100 mV and the repolarizing potential was −50 mV. At both these negative voltages, there was little Mg^{2+} block, as suggested by the results of Fig. 1 C. On the other hand, a steady-state inward current was observed in the presence of 10 mM $[Mg^{2+}]_i$, but not in the absence of Mg^{2+}, suggesting that Mg^{2+} activated mslo1 channels at these negative voltages even though the block was largely relieved. Unlike the Mg^{2+} block, the activation of mslo1 channels by Mg^{2+} seems to be insensitive to voltage, resulting in a parallel shift of G-V relations on the voltage axis without affecting the slope (Fig. 1 B). Such insensitivity to voltage in the change of G-V relations is more prominent when we compare the results at 0 and 110 μM $[Ca^{2+}]_i$. The voltage of half-maximum activation ($V_{1/2}$) at 0 $[Ca^{2+}]_i$ is ~170 mV more positive than at 110 μM $[Ca^{2+}]_i$ (Fig. 1 B). Nevertheless, 10 mM Mg^{2+} shifts the G-V relation to the left on the voltage axis with a similar amount at both $[Ca^{2+}]_i$'s (Figs. 1 B and 2 C). This result indicates that the binding of Mg^{2+} that activates the channel is not sensitive to membrane potential, obviously in contrast to the voltage dependence of Mg^{2+} binding in channel block. Therefore, the Mg^{2+} ion that activates the channel cannot be the Mg^{2+} ion that blocks it. Results in later sections also support the conclusion that Mg^{2+} affects the gating and permeation through distinct binding sites and mechanisms. In the following, we will primarily focus on the effects of Mg^{2+} on voltage- and Ca^{2+}-dependent activation of the channel without considering the Mg^{2+} block.

The Activation by Mg^{2+} Is Not Directly Affected by Voltage or Ca^{2+}

Mg^{2+} activates mslo1 channels by shifting G-V relations to the left on the voltage axis (Fig. 1 B and Fig. 2),

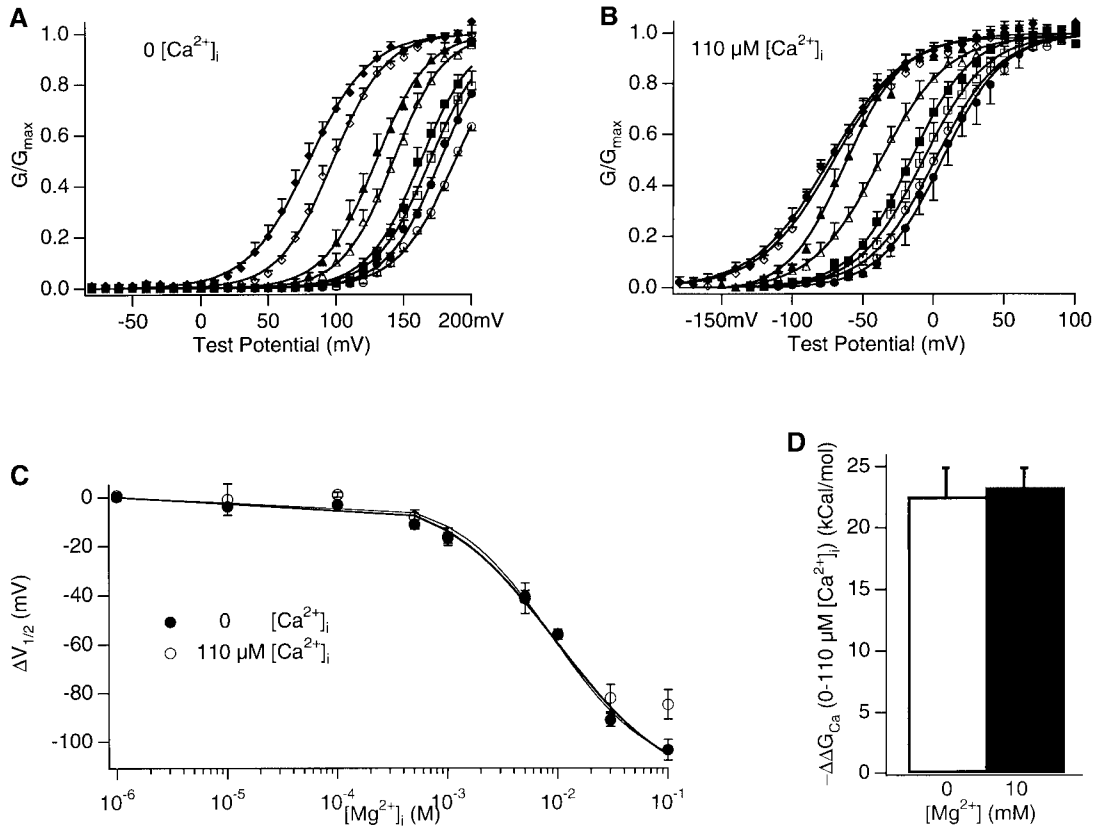

FIGURE 2. G-V relations in the presence of 0∼100 mM $[Mg^{2+}]_i$ at 0 (A) or 110 μM $[Ca^{2+}]_i$ (B). The symbols represent $[Mg^{2+}]_i$ at (in mM) 0 (open circle), 0.1 (closed circle), 0.5 (open square), 1 (closed square), 5 (open triangle), 10 (closed triangle), 30 (open diamond), and 100 (closed diamond). G-V relations from a number (n) of patches at each $[Mg^{2+}]_i$ are averaged and plotted. Smooth curves are Boltzmann fits to averaged G-V relations. At 0 $[Ca^{2+}]_i$ (A), z and $V_{1/2}$ at various $[Mg^{2+}]_i$ (mM) are as follows for 0, 1.17, 186.4 mV (n = 12); for 0.1, 1.30, 177.0 mV (n = 4); for 0.5, 1.26, 169.5 mV (n = 4); for 1, 1.30, 162.7 (n = 4); for 5, 1.36, 142.4 mV (n = 4); for 10, 1.32, 129.6 mV (n = 4); for 30, 1.30, 97.76 mV (n = 7); and for 100, 1.13, 80.1 mV (n = 8), respectively. At 110 μM $[Ca^{2+}]_i$ (B), z and $V_{1/2}$ at various $[Mg^{2+}]_i$ (mM) are as follows: for 0, 1.10, 1.2 mV (n = 10); for 0.1, 1.17, 5.8 mV (n = 5); for 0.5, 1.12, −7.6 mV (n = 6); for 1: 1.20, -16.0 (n = 6); for 5, 1.06, −38.2 mV (n = 5); for 10, 1.26, −62.5 mV (n = 4); for 30, 0.97,−70.4 mV (n = 4); and for 100, 0.95, −73.4 mV (n = 4), respectively. (C) Left shifts of G-V relations on the voltage axis caused by various $[Mg^{2+}]_i$ at 0 and 110 μM $[Ca^{2+}]_i$. $\Delta V_{1/2}$ = ($V_{1/2}$ at each $[Mg^{2+}]_i$ − $V_{1/2}$ at 0 $[Mg^{2+}]_i$) obtained from n = 4 patches at 0 $[Ca^{2+}]_i$ and n = 6 patches at 110 μM $[Ca^{2+}]_i$ are averaged and then plotted. The smooth curves are fits of Eq. 1 to data at 0 $[Ca^{2+}]_i$ with z = 1.30. For the thick curve, m is fixed at 4, K_C = 15.0 mM, K_O = 3.6 mM. For the thin curve, m is let free in the fit and is 1.94, K_C = 45.7 mM, K_O = 2.12 mM. (D) Changes in the activation energy provided by Ca^{2+} binding as the result of an increased $[Ca^{2+}]_i$ from 0 to 110 μM in the absence or presence of 10 mM $[Mg^{2+}]_i$. $-\Delta\Delta G_{Ca}$ = ($zV_{1/2}$ at 0 $[Ca^{2+}]_i$ − $zV_{1/2}$ at 110 μM $[Ca^{2+}]_i$)eN, where e is elementary charge and N is Avogadro's number. Averaged from n = 4 patches.

which is similar to the Ca^{2+}-dependent activation of mslo1 channels (Marty, 1981; McManus and Magleby, 1991; Pallotta et al., 1981; Adelman et al., 1992; Cui et al., 1997). It has been demonstrated that each of the four mslo1 channel subunits contains a high affinity Ca^{2+} binding site in the tail domain, which includes the Ca^{2+} bowl that contains repetitive negatively charged amino acids (Shen et al., 1994; Moss et al., 1996; Schreiber et al., 1999; Bian et al., 2001). The dissociation constant of Ca^{2+} binding is estimated to be ∼1 or 10 μM when the channel is open or closed, respectively (Cox et al., 1997a). Ca^{2+} activates the channel by preferentially binding to and stabilizing the open states, which can be described by allosteric mechanisms such as the MWC model (Monod et al., 1965; McManus and Magleby, 1991; Cox et al., 1997a; Horrigan et al., 1999). Then, what is the mechanism of activation of the mslo1 channel by Mg^{2+}? To answer this question, we first investigated whether Mg^{2+} activates the channel by affecting the Ca^{2+}-dependent activation.

Mg^{2+} might activate the mslo1 channel by affecting the Ca^{2+}-dependent activation in two ways: (1) by binding to the same high affinity Ca^{2+} binding sites to activate the channel, or (2) by binding to other separate sites to increase Ca^{2+} affinity or efficacy. In either case, Ca^{2+} should also affect the Mg^{2+}-dependent activation reciprocally (Colquhoun, 1998). Contrary to this prediction, Fig. 1 B shows that either in the absence of (at

0 $[Ca^{2+}]_i$; MATERIALS AND METHODS) or nearly saturated Ca^{2+} binding (at 110 μM $[Ca^{2+}]_i$; Cox et al., 1997a) 10 mM $[Mg^{2+}]_i$ shifted the G-V relation on the voltage axis by a similar amount. The activation of the channel at other $[Mg^{2+}]_i$'s is also not affected whether the high affinity Ca^{2+} binding sites are empty (at 0 $[Ca^{2+}]_i$) or saturated with Ca^{2+} (at 110 μM $[Ca^{2+}]_i$) (Fig. 2). Fig. 2 (A and B) shows that at both $[Ca^{2+}]_i$'s, increasing $[Mg^{2+}]_i$ from 0.1 to 100 mM gradually shifts the G-V relation to the left on the voltage axis without affecting the slope. The averaged amounts of G-V shift ($\Delta V_{1/2}$) at both $[Ca^{2+}]_i$'s are plotted versus $[Mg^{2+}]_i$ in Fig. 2 C. Clearly, despite the large differences in $[Ca^{2+}]_i$ and in the voltage range of G-V curves at the two $[Ca^{2+}]_i$'s (Fig. 2, A and B), $\Delta V_{1/2}$ is similar at various $[Mg^{2+}]_i$ from 1 μM up to 30 mM (Fig. 2 C).

The above results demonstrate that Ca^{2+} does not affect Mg^{2+}-dependent activation of mslo1 channels. Conversely, it can be also directly demonstrated that Mg^{2+} does not affect the Ca^{2+}-dependent activation. Recently, it has been shown that the free energy contributions to mslo1 channel activation provided by voltage (ΔG_V) and by Ca^{2+} binding (ΔG_{Ca}) are simply additive (Cui and Aldrich, 2000). This property dictates that, in response to an increase in $[Ca^{2+}]_i$, the shift of G-V relations on the voltage axis is simply determined by the change in the contribution of Ca^{2+} binding to the free energy of channel opening, $\Delta\Delta G_{Ca}$ ($\Delta\Delta G_{Ca}$ = ΔG_{Ca} at the high $[Ca^{2+}]_i$ − ΔG_{Ca} at the low $[Ca^{2+}]_i$). As a consequence, $\Delta\Delta G_{Ca}$ can be directly measured from the properties of the G-V relation: $\Delta\Delta G_{Ca} = \Delta(zV_{1/2})$, where $\Delta(zV_{1/2}) = zV_{1/2}$ at the high $[Ca^{2+}]_i$ − $zV_{1/2}$ at the low $[Ca^{2+}]_i$ (Cui and Aldrich, 2000). The parameters z and $V_{1/2}$ are obtained from the Boltzmann fit to G-V relations (Fig. 1, legend). With this method, we have compared the contribution of Ca^{2+} binding to the free energy of mslo1 channel opening in the presence or absence of 10 mM $[Mg^{2+}]_i$ (Fig. 2 D). When $[Ca^{2+}]_i$ increases from 0 μM to the near-saturating 110 μM in the absence of intracellular Mg^{2+}, the G-V relation shifts ~170 mV to the left on the voltage axis (Fig. 1 B). From such results, it is calculated that, at near-saturating $[Ca^{2+}]_i$, Ca^{2+} binding contributes −22.6 ± 2.2 kcal/mol to the free energy of mslo1 channel opening (Fig. 2 D). Likewise, in the presence of 10 mM $[Mg^{2+}]_i$, the G-V relation shifts a similar amount on voltage axis with the same $[Ca^{2+}]_i$ increases without significantly changing the slope (Figs. 1 B and 2 B), and the free energy of Ca^{2+} binding contributed to channel opening is −23.3 ± 1.8 kcal/mol, similar to that in the absence of Mg^{2+} (Fig. 2 D). This result indicates that Mg^{2+} does not affect the contribution of Ca^{2+} binding to the free energy of mslo1 channel opening. In other words, neither the affinity of Ca^{2+} binding nor the efficacy of Ca^{2+}-dependent activation is affected by Mg^{2+}.

The Mg^{2+} Binding Site Is Located in the Core Domain

Since Mg^{2+} activates the channel without affecting Ca^{2+}-dependent activation, the Mg^{2+} binding sites must be distinct from the high affinity Ca^{2+} binding sites located in the tail domain (Moss et al., 1996; Schreiber et al., 1999; Bian et al., 2001). Recordings of the mslo3 channel and the channel resulting from the coexpression of the mslo1 core and mslo3 tail (Fig. 3) confirm this conclusion. The tail domain of mslo3 lacks the Ca^{2+} bowl and is not sensitive to Ca^{2+} (Fig. 3 A; Schreiber et al., 1998). Similar to mslo1 channels, the mslo3 channel was blocked by 10 mM $[Mg^{2+}]_i$ (Fig. 3 B), and the block was voltage-dependent (the ratio $I_{[Mg^{2+}]i = 0}/I_{[Mg^{2+}]i = 10\ mM}$ for the peak current at 130 mV was 3.3, but for the tail current at −50 mV was 1.0). However, Mg^{2+} did not affect its activation (Fig. 3 C), suggesting that mslo3 lacks the Mg^{2+} binding sites for activation, although Mg^{2+} can block the channel. To test whether the Mg^{2+} binding sites for activation are located in the tail or the core domain, we recorded currents from channels expressed from a RNA mixture of the mslo1 core domain and the mslo3 tail domain (Fig. 3 D; Wei et al., 1994; Schreiber et al., 1999). This channel is not sensitive to the $[Ca^{2+}]_i$ change from 0 to 110 μM due to the lack of high affinity Ca^{2+} binding sites (Schreiber et al., 1999). If the Mg^{2+} binding sites for activation are also located in the tail domain, then this channel should not be activated by Mg^{2+} since its tail is derived from the Mg^{2+}-insensitive mslo3 and apparently should lack the binding sites. However, 10 mM $[Mg^{2+}]_i$ activated this channel, shifting the G-V relation to the left on the voltage axis by ~56 mV (Fig. 3 F), similar to that in the activation of mslo1 (Figs. 1 and 2). This result indicates that the core domain of mslo1 confers Mg^{2+} sensitivity to the chimeric channel. Therefore, the Mg^{2+} binding sites for activation are most likely located in the mslo1 core, which are distinct from the high affinity Ca^{2+} binding sites.

The Allosteric Mechanism of Mg^{2+}-dependent Activation

Fig. 4 A shows the Mg^{2+} dose–response curves of the steady-state open probability (G/G_{max}) at 0 $[Ca^{2+}]_i$ and various voltages. At all voltages, the open probability increases with $[Mg^{2+}]_i$. The Mg^{2+}-dependent component of the open probability, G(Mg), is fitted with the Hill equation. Fig. 4 C plots the Hill coefficient from the fits. At most voltages, the Hill coefficient is between 1 and 2. Since Hill coefficient indicates the lower limit for the number of positively cooperating binding sites (Stryer, 1995), it is clear that the mslo1 channel has at least two Mg^{2+} binding sites for activation. The Hill coefficient in Fig. 4 C shows a weak voltage dependence that peaks at ~80–120 mV. The maximum Hill coefficient of Mg^{2+} dependence is obviously smaller than that of Ca^{2+} dependence (see Fig. 6E), which arises

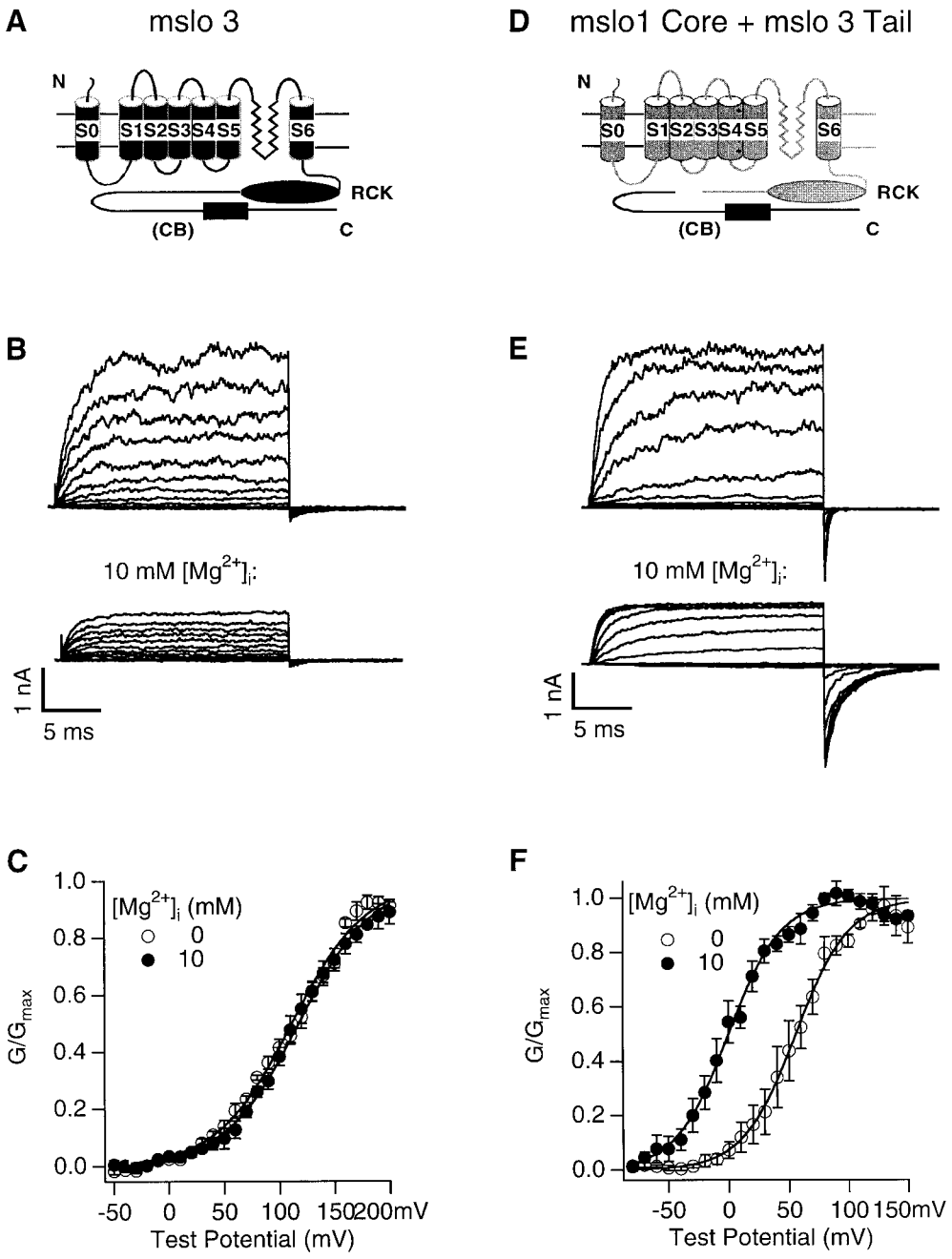

FIGURE 3. Mg^{2+} effects on mslo3 channels or the channels from coexpression of the mslo1 core and mslo3 tail. (A and D) Schematic representation of mslo3 (A) and the mslo1 core (light) and the mslo3 tail (dark) (D). S0–S6 are transmembrane segments, RCK indicates the RCK domain (Jiang et al., 2001), and CB signifies the lack of calcium bowl. (B) mslo3 currents from an inside-out patch in the absence (top) or presence (bottom) of 10 mM $[Mg^{2+}]_i$. The holding and repolarizing potentials are −50 mV. The test potentials are from −80 to 200 mV with 20-mV increment. $[Ca^{2+}]_i = 0$. (C) G-V relations of mslo3 channels in the absence or presence of 10 mM $[Mg^{2+}]_i$. $[Ca^{2+}]_i = 0$. G-V curves are averaged from $n = 6$ patches, and then fitted with the Boltzmann equation (smooth lines) with z = 0.76 and $V_{1/2}$ = 111.3 mV at 0 $[Mg^{2+}]_i$ and z = 0.76 and $V_{1/2}$ = 117.6 mV at 10 mM $[Mg^{2+}]_i$, respectively. (E) Currents from an inside-out patch that coexpresses the mslo1 core and mslo3 tail in the absence (top) or presence (bottom) of 10 mM $[Mg^{2+}]_i$. The voltage protocol is the same as in B except that the test potential stops at 140 mV. $[Ca^{2+}]_i = 1.1$ μM. (F) G-V relations of channels from the coexpression of the mslo1 core and mslo3 tail in the absence or presence of 10 mM $[Mg^{2+}]_i$. $[Ca^{2+}]_i = 1.1$ μM. Smooth lines are fits of the Boltzmann equation with z = 1.14 and $V_{1/2}$ = 55.9 mV at 0 $[Mg^{2+}]_i$ and z = 1.16 and $V_{1/2}$ = 0.2 mV at 10 mM $[Mg^{2+}]_i$, respectively. $n = 4$ patches.

from the binding of Ca^{2+} to four high affinity Ca^{2+} sites that progressively promotes channel opening (Cox et al., 1997a; Cui et al., 1997). The smaller Hill coefficient of Mg^{2+}-dependent activation indicates either of the following possibilities. First, the channel has fewer Mg^{2+} binding sites, possibly two, considering the symmetry of the tetrameric channel (Jiang et al., 2001; Zagotta, 2001). Second, as for Ca^{2+} binding, the channel has four Mg^{2+} sites, one on each subunit (Shen et al., 1994), but the binding of each Mg^{2+} promotes channel opening less than the binding of each Ca^{2+} to the high affinity Ca^{2+} site.

The apparent K_d from the Hill equation fits clearly shows a voltage dependence (Fig. 4 D). At 0 mV, the apparent K_d is 242.3 mM, whereas at 180 mV, it is 1.6 mM. Such apparent voltage dependence appears to be in

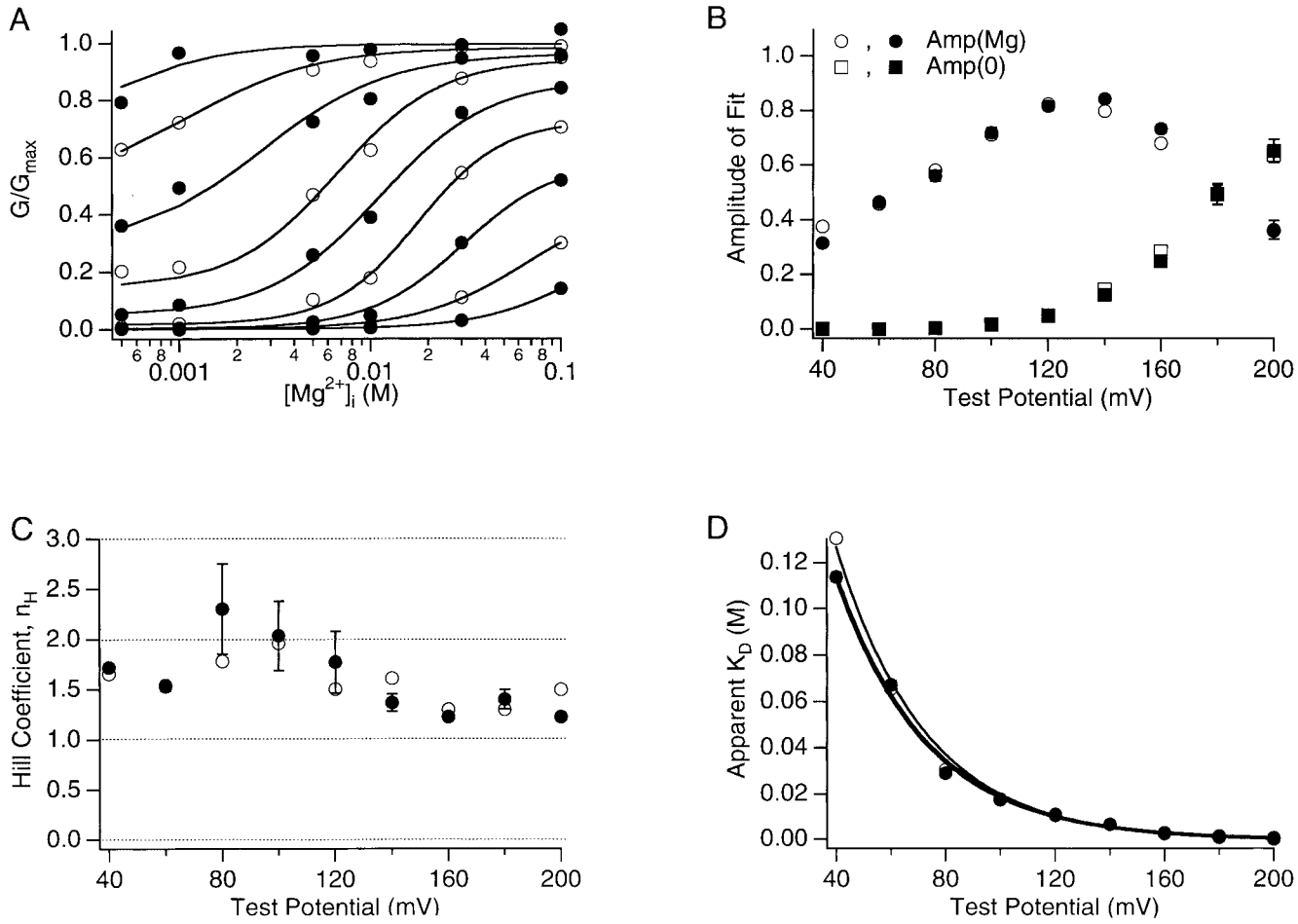

FIGURE 4. Mg^{2+} dependence of mslo1 currents. (A) Average normalized G-V relations at 0 $[Ca^{2+}]_i$ and the following $[Mg^{2+}]_i$: 0, 0.1, 0.5, 1, 5, 10, 30, and 100 mM were transformed to dose–response curves as displayed (data at 0 and 0.1 mM $[Mg^{2+}]_i$ is not shown on the logarithm scale). Alternating closed and open circles represent the dose–response curves (ascending right to left) at different voltages between 40 and 200 mV in 20-mV increments. Smooth curves represent fits to the Hill equation ($G/G_{max} = Amp(Mg)/(1 + (K_d/[Mg^{2+}]_i)^{nH}) + Amp(0)$), where n_H is Hill coefficient, K_d is the apparent Mg^{2+} dissociation constant, $Amp(0) = G/G_{max}$ at 0 $[Mg^{2+}]_i$, and $Amp(Mg)$ is the Mg^{2+}-dependent component of G/G_{max}. (B–D) The amplitudes, Hill coefficient, and apparent dissociation constant determined from fits to the Hill equation are plotted versus voltage. Open symbols represent parameters determined from the fits in A. Closed symbols represent the mean values from four experiments. In D, solid lines are fits with the function $K_d(V) = K_d(0)\exp(zeV/kT)$. The thin line fits the results determined in A, $K_d(0) = 378.8$ mM and $z = 0.77$. The thick line fits the mean results from four experiments, $K_d(0) = 242.3$ mM and $z = 0.77$.

contrast to the results in Fig. 1 B and Fig. 2 that the shifts of G-V relations caused by Mg^{2+} are insensitive to voltage. In other words, the results in Fig. 1 B and Fig. 2 indicate that the binding of Mg^{2+} is not directly dependent on voltage, whereas the apparent K_d in Fig. 4 indicates that it is influenced by voltage. These results can be reconciled by concluding that the binding of Mg^{2+} must be dependent on the conformation of the channel but not on voltage per se. The Mg^{2+} affinity is higher at the open conformation than at the closed. At more positive voltages, more channels are open, therefore, the apparent K_d decreases with voltage. This mechanism of cooperative Mg^{2+} binding is described by the model for allosteric transitions (Scheme I), which is similar to the mechanism of Ca^{2+}-dependent activation of the channel (Cox et al., 1997a; Cui et al., 1997).

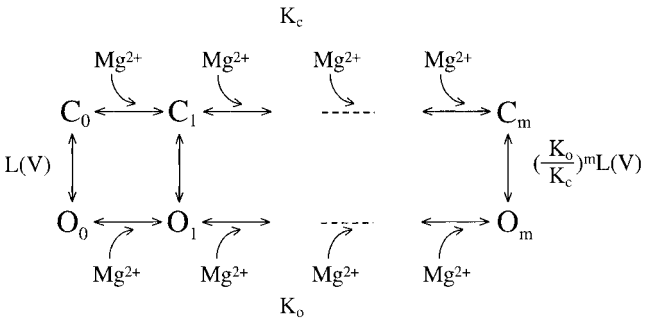

(SCHEME I)

In Scheme I, each channel has m Mg^{2+} binding sites. K_C and K_O are the microscopic dissociation constants of Mg^{2+} at closed (C) and open (O) conformation, respectively. L(V) is the equilibrium constant between C_0 and O_0, the closed and open conformation with no Mg^{2+} bound. In Fig. 2 C, the shift of G-V relations versus $[Mg^{2+}]_i$ at 0 $[Ca^{2+}]_i$ is fitted with Eq. 1 derived from Scheme I (Cui and Aldrich, 2000),

$$V_{1/2} = \frac{kT}{ze} m \ln\left(\frac{1 + \frac{[Mg^{2+}]_i}{K_C}}{1 + \frac{[Mg^{2+}]_i}{K_O}}\right). \quad (1)$$

The fit results in a number of Mg^{2+} binding sites m = 2 when it is let free, K_C and K_O being 45.7 and 2.12 mM, respectively. The model fits the data equally well (Fig. 2 C) if the number of Mg^{2+} binding sites is assumed to be four, resulting in a K_C and K_O of 15.0 mM and 3.6 mM, respectively.

Ca^{2+} Also Binds to the Low Affinity Mg^{2+} Sites of Activation

In the above experiments, we added $MgCl_2$ to the basal internal solution to vary $[Mg^{2+}]_i$ (MATERIALS AND METHODS). With such a method, besides the change of $[Mg^{2+}]_i$, $[Cl^-]_i$ and the osmolarity of intracellular solution were also changed. To examine if increased intracellular Cl^- or osmolarity contribute to our observed mslo1 channel activation, we compared the G-V relations in the basal internal solution with or without the addition of 20 mM KCl. Fig. 5 A shows that the addition of 20 mM KCl caused 6-mV shift of the G-V relation to a more positive voltage range. Such change is much smaller and to an opposite direction as compared with the changes caused by addition of 10 mM $MgCl_2$ (Fig. 1 B). In fact, such a small change in G-V relations is within the variability of mslo1 channels, and is often observed among experiments even under identical conditions. This result indicates that the increase of intracellular $[K^+]_i$ (from 142 to 162 mM), $[Cl^-]_i$ (from 2 to 22 mM), or osmolarity had little effect on the activation of mslo1 channels under our experimental condition.

Then, are these sites only selective to Mg^{2+}, or does Ca^{2+} also bind to them? It has been well- known that the activation of mslo1 channels is not saturated at $[Ca^{2+}]_i$, even above 1 mM (Wei et al., 1994; Cui et al., 1997) although the dissociation constants of the high affinity Ca^{2+} binding sites are estimated to be 1 and 10 μM at open and closed conformations, respectively (Cox et al., 1997a). The continued activation of mslo1 channels at $[Ca^{2+}]_i$ above 110 μM was suggested to derive from a binding site nonspecific for divalent cations (Wei et al., 1994). It was also reported that Ca^{2+} sensitivity persisted in mslo1 channels when the Ca^{2+} bowl was substituted with sequences from the mslo3 tail, suggesting that a second class of Ca^{2+} binding sites might exist (Schreiber et al., 1999). As shown in Fig. 5 B, adding 10 mM $[Ca^{2+}]_i$ to the internal solution that contained 110 μM $[Ca^{2+}]_i$ shifted the G-V relation to more negative voltages by ~75 mV. This effect is similar to that of 10 mM $[Mg^{2+}]_i$ at 110 μM $[Ca^{2+}]_i$ (Fig. 1 B), suggesting that Ca^{2+} may bind to the Mg^{2+} binding sites and activate mslo1 channels to the same extent. 10 mM $[Ca^{2+}]_i$ also activates the chimera channel expressed from the mix of mslo1 core and mslo3 tail, shifting the G-V relation by −70 mV (unpublished data). This chimera channel lacked the Ca^{2+} sensitivity when $[Ca^{2+}]_i$ was lower than

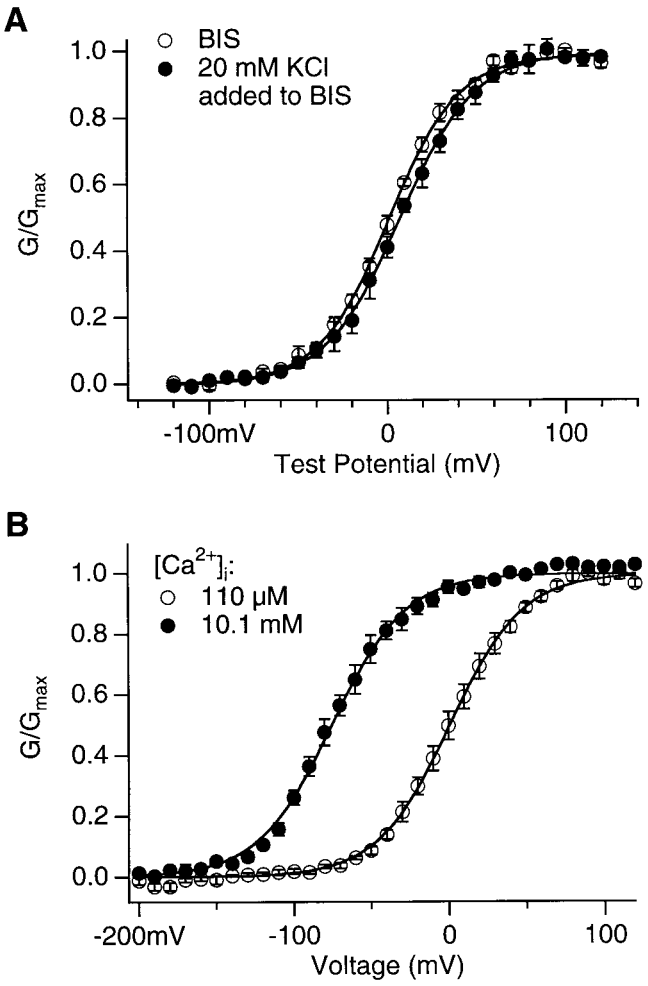

FIGURE 5. The effects of $[KCl]_i$ and high $[Ca^{2+}]_i$ on the activation of mslo1 channels. (A) G-V relations of mslo1 channels with or without 20 mM KCl added to the basal internal solution (BIS; MATERIALS AND METHODS). The total $[Cl^-]_i$ is 22 mM and 2 mM, respectively. The total $[K^+]_i$ is 162 and 142 mM, respectively. $[Ca^{2+}]_i$ = 110 μM. The data was averaged from the results of $n = 4$ patches. Smooth lines are Boltzmann fits to data. With BIS, z = 1.29 and $V_{1/2}$ = 1.1 mV. With 20 mM $[KCl]_i$ added to BIS, z = 1.21 and $V_{1/2}$ = 7.2 mV. (B) G-V relations of mslo1 channels at 110 μM or 10.1 mM $[Ca^{2+}]_i$. Smooth lines are Boltzmann fits to data. At 110 μM $[Ca^{2+}]_i$, z = 1.09 and $V_{1/2}$ = 1.0 mV. At 10.1 mM $[Ca^{2+}]_i$, z = 1.06 and $V_{1/2}$ = −75.1 mV.

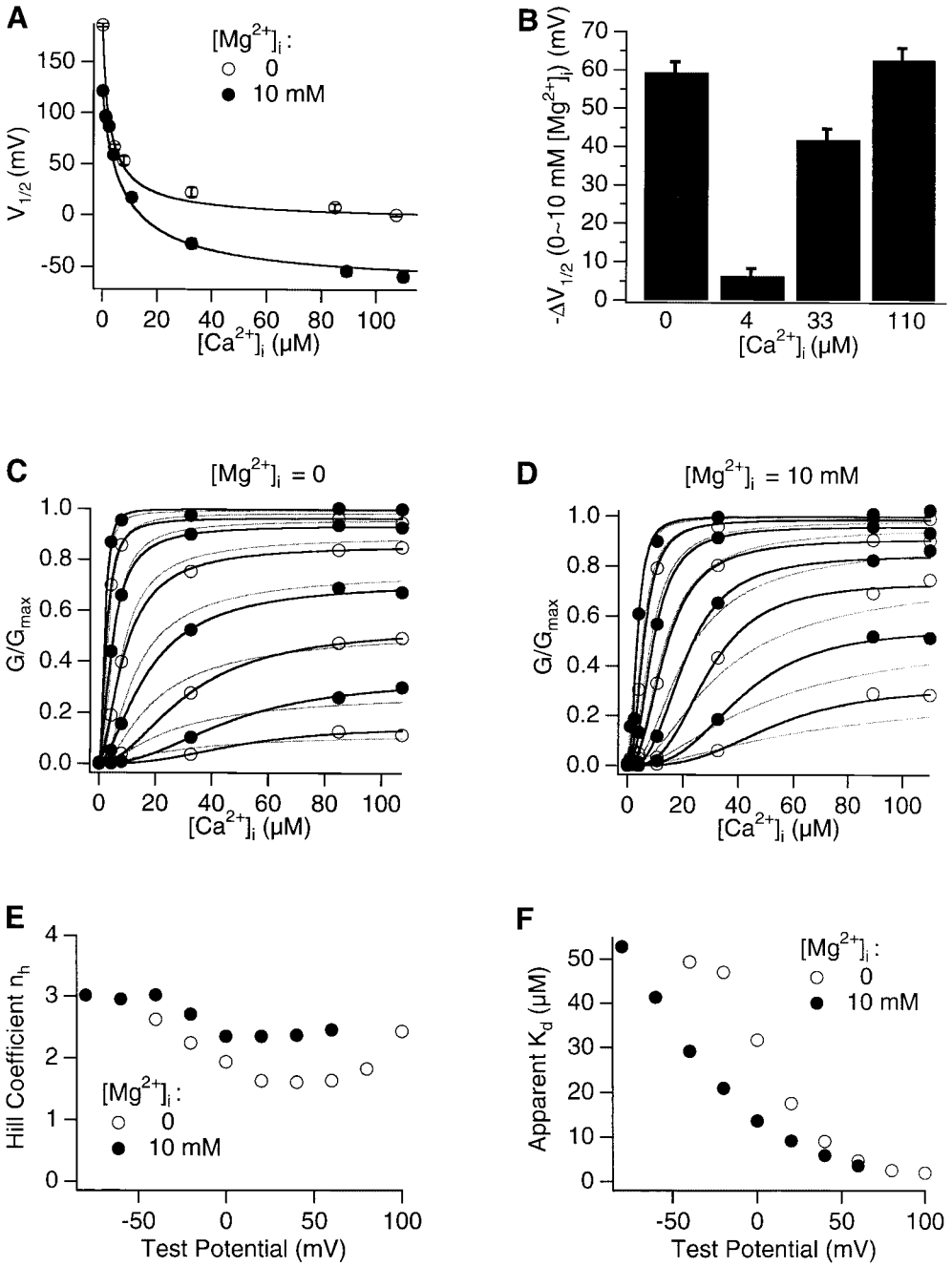

FIGURE 6. Effects of intracellular Mg^{2+} on Ca^{2+}-dependent activation. (A) $V_{1/2}$ of G-V relations at various $[Ca^{2+}]_i$ in the presence or absence of 10 mM $[Mg^{2+}]_i$. The smooth lines are fits of Eq. 6 to data. Each data point is averaged from n = ~4–8 patches. (B) The difference in $V_{1/2}$ in the presence or absence of 10 mM $[Mg^{2+}]_i$. At each $[Ca^{2+}]_i$, $\Delta V_{1/2}$ = ($V_{1/2}$ at 10 mM $[Mg^{2+}]_i$ − $V_{1/2}$ at 0 $[Mg^{2+}]_i$), averaged from n = 4–6 patches. (C) and D) $[Ca^{2+}]_i$ dependence of normalized conductance in the absence (C) or presence (D) of 10 mM $[Mg^{2+}]_i$. Each data point is averaged from n = 4–8 patches. Alternating open and closed circles represent the curves (ascending right to left) at different voltages between −40 and 100 mV (C) or between −80 and 60 mV (D) in 20-mV increments. Dark or light smooth curves represent fits to the Hill equation or to Eqs. 2–5 (Scheme II), respectively. (E and F) Hill coefficient (E) and apparent K_d (F) obtained from fits of data in the presence or absence of 10 mM $[Mg^{2+}]_i$ to the Hill equation.

110 μM because of the absence of the high affinity Ca^{2+} sites (Schreiber et al., 1999). Therefore, its activation by 10 mM $[Ca^{2+}]_i$ is most likely through the low affinity Mg^{2+}/Ca^{2+} binding sites. Based on extensive analysis of mslo1 channel activation in the presence of high $[Ca^{2+}]$ (1–100 mM), Zhang et al. (2001) also concluded that Ca^{2+} at high concentrations activates the channel through the low affinity Mg^{2+}/Ca^{2+} binding sites. It is worth pointing out that these results do not exclude the possibility that Ca^{2+} at 10 mM concentration may activate the channel by binding to yet another class of low affinity Ca^{2+} sites that differ from both the high affinity Ca^{2+} sites and the Mg^{2+} sites. However, we consider it a less likely mechanism.

Mg^{2+} Competitively Antagonizes Ca^{2+}-dependent Activation

When the high affinity Ca^{2+} binding sites in mslo1 channels are either empty of ($[Ca^{2+}]_i$ = 0) or nearly saturated by Ca^{2+} ($[Ca^{2+}]_i$ = 110 μM), 10 mM $[Mg^{2+}]_i$ shifts the G-V by about −65 mV (Figs. 1 and 2). These results indicate that the binding of Mg^{2+} to the low affinity Mg^{2+}/Ca^{2+} sites has no effect on Ca^{2+}-dependent activation via the high affinity Ca^{2+} sites. However, when $[Ca^{2+}]_i$ was between 0 μM and the saturating 110

μM, 10 mM $[Mg^{2+}]_i$ shifted the G-V to less extents (Fig. 6, A and B). The amount of G-V shift caused by 10 mM $[Mg^{2+}]_i$ dropped to <5 mV at 4 μM $[Ca^{2+}]_i$, and then increases at higher $[Ca^{2+}]_i$ (Fig. 6 B). Such a Ca^{2+} dependence of the Mg^{2+} induced G-V shift indicates that, besides activating the channel by binding to the low affinity Mg^{2+}/Ca^{2+} sites, Mg^{2+} also interferes with Ca^{2+} binding at the high affinity Ca^{2+} sites. Such interference is consistent with the mechanism that Mg^{2+} competitively binds to the high affinity Ca^{2+} sites and antagonizes Ca^{2+}-dependent activation. Thus, Mg^{2+} may affect channel activation by two separate mechanisms. Mg^{2+} binds to the low affinity Mg^{2+}/Ca^{2+} sites and activates the channel, shifting the G-V to the left on voltage axis. Meanwhile, Mg^{2+} also binds to the high affinity Ca^{2+} site and prevents Ca^{2+} from binding to the same site. Unlike Ca^{2+}, Mg^{2+} may bind to the high affinity Ca^{2+} sites with an affinity that does not depend on the conformation of the channel and, thus, unable to activate the channel. Therefore, in the absence of Ca^{2+} ($[Ca^{2+}]_i = 0$) the binding of Mg^{2+} to the high affinity Ca^{2+} sites has no effect on channel activation. The net effect of Mg^{2+} on channel activation may derive only from its binding to the low affinity Mg^{2+}/Ca^{2+} sites. At low $[Ca^{2+}]_i$, due to the competition from Mg^{2+}, Ca^{2+} activates the channel to a lesser extent than it would have in the absence of Mg^{2+}. The net effect on the G-V by adding Mg^{2+} to the low $[Ca^{2+}]_i$ solution would be the left shift derived from the binding of Mg^{2+} to low affinity Mg^{2+}/Ca^{2+} sites minus the lost Ca^{2+}-dependent activation due to the competitive binding of Mg^{2+} to high affinity Ca^{2+} sites. This net leftward shift is less than the Mg^{2+} induced G-V shift at 0 $[Ca^{2+}]_i$. As $[Ca^{2+}]_i$ increases, Mg^{2+} is less competitive in binding high affinity Ca^{2+} sites, and this results in reduced losses of Ca^{2+}-dependent activation. The loss of Ca^{2+}-dependent activation becomes zero at the saturating $[Ca^{2+}]_i$, where the Mg^{2+} competition is negligible. Thus, the net left-ward shift of G-V increases with $[Ca^{2+}]_i$, and at saturating $[Ca^{2+}]_i$ it becomes the same as at 0 $[Ca^{2+}]_i$.

If the above mechanism is correct, the competitive inhibition of Ca^{2+}-dependent activation by Mg^{2+} should depend on the ratio of $[Mg^{2+}]_i/[Ca^{2+}]_i$. At 10 mM $[Mg^{2+}]_i$ the competitive inhibition becomes negligible when $[Ca^{2+}]_i$ is increased to 110 μM. However, at the same $[Ca^{2+}]_i$ of 110 μM the competitive inhibition should become evident again if $[Mg^{2+}]_i$ is increased. This prediction is confirmed by the results shown in Fig. 2. The G-V shift caused by $[Mg^{2+}]_i$ up to 10 mM is the same at 0 and 110 μM $[Ca^{2+}]_i$. However, at 30 mM $[Mg^{2+}]_i$, the G-V shifts less at 110 μM $[Ca^{2+}]_i$ than at 0 $[Ca^{2+}]_i$ (Fig. 2 C). At these two $[Ca^{2+}]_i$'s, the difference in G-V shift caused by 100 mM $[Mg^{2+}]_i$ is even larger (Fig. 2 C), indicating the loss of Ca^{2+}-dependent activation caused by the competitive inhibition. The above mechanism is also supported by the result that the Mg^{2+} induced G-V shift of the channel from the coexpression of mslo1 core and mslo3 tail is not affected whether $[Ca^{2+}]_i$ is 0 or 1.1 μM (Fig. 3).

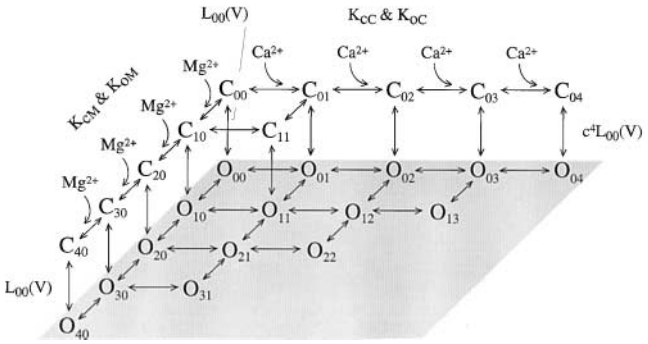

(SCHEME II)

Scheme II[2] shows a kinetic model of such competitive inhibition. In this scheme, Ca^{2+}-dependent activation of the mslo1 channel follows the MWC model (Cox et al., 1997a). The four high affinity Ca^{2+} binding sites can be occupied by either Mg^{2+} or Ca^{2+}. The affinity for Ca^{2+} is higher at open states (dissociation constant: K_{oC}) than at closed states (K_{cC}), thus, the binding of Ca^{2+} activates the channel. On the other hand, the binding of Mg^{2+} does not affect channel gating because the affinity for Mg^{2+} is the same at both open and closed states ($K_{oM} = K_{cM}$). The occupancy of Mg^{2+} on a site prevents the binding of Ca^{2+} to the same site, thereby Mg^{2+} competitively inhibits Ca^{2+}-dependent activation. Taken together, Scheme II describes voltage and Ca^{2+}-dependent activation and the competitive inhibition by Mg^{2+}, whereas Scheme I describes voltage and Mg^{2+}-dependent activation of the mslo1 channel. Since Mg^{2+}-dependent activation is not directly affected by voltage or Ca^{2+} but linked to voltage and Ca^{2+}-dependent activation through the transition between closed and open conformations, the energy provided by Mg^{2+} and Ca^{2+} binding and voltage are additive in activating the channel (Cui and Aldrich, 2000). The open probability of mslo1 channels, therefore, is described by:

$$P_o = \frac{1}{1 + e^{\frac{\Delta G_V + \Delta G_{Ca} + \Delta G_{Mg}}{kT}}}, \qquad (2)$$

[2]Scheme II. The competitive inhibition of Ca^{2+}-dependent activation by Mg^{2+}. Each open state in the bottom layer has a corresponding closed state at the top layer but not all of the closed states and transitions are shown in the interest of clarity. $L_{00}(V)$ is the equilibrium constant between the open and closed conformation in the absence of Ca^{2+} or Mg^{2+} binding (C_{00}-O_{00}). K_{cC}, K_{oC}, K_{cM}, and K_{oM} are described in the text. $c = K_{oC}/K_{cC}$. The value of parameters is obtained from the model fits to data in Fig. 6 (A, C, and D). $L_{00}(V) = 15{,}000\exp(-1.32eV/kT)$, $K_{cC} = 8.7$ μM, $K_{oC} = 0.75$ μM, and $K_{cM} = K_{oM} = 5.6$ mM.

where

$$\Delta G_V = kT \ln(L_{00}(V)), \quad (3)$$

$$\Delta G_{Ca} = 4kT \ln\left(\frac{1 + \frac{[Ca^{2+}]_i}{K_{cC}} + \frac{[Mg^{2+}]_i}{K_{cM}}}{1 + \frac{[Ca^{2+}]_i}{K_{oC}} + \frac{[Mg^{2+}]_i}{K_{oM}}}\right), \quad (4)$$

and

$$\Delta G_{Mg} = 4kT \ln\left(\frac{1 + \frac{[Mg^{2+}]_i}{K_C}}{1 + \frac{[Mg^{2+}]_i}{K_O}}\right). \quad (5)$$

The position of the G-V relation on voltage axis in the presence of both intracellular Ca^{2+} and Mg^{2+} is determined by:

$$V_{1/2} = V_{1/2}(00) + \frac{4kT}{ze}\left\{\ln\left(\frac{1 + \frac{[Ca^{2+}]_i}{K_{cC}} + \frac{[Mg^{2+}]_i}{K_{cM}}}{1 + \frac{[Ca^{2+}]_i}{K_{oC}} + \frac{[Mg^{2+}]_i}{K_{oM}}}\right) + \ln\left(\frac{1 + \frac{[Mg^{2+}]_i}{K_C}}{1 + \frac{[Mg^{2+}]_i}{K_O}}\right)\right\}. \quad (6)$$

where $V_{1/2}(00)$ is the $V_{1/2}$ at 0 $[Ca^{2+}]_i$ and $[Mg^{2+}]_i$. Such combination of Schemes I and II can account for our experimental data at various $[Ca^{2+}]_i$, $[Mg^{2+}]_i$, and voltages (Fig. 6, A–D) with the same parameters (Fig. 2, legend, and Scheme II footnote).

The above results demonstrate that intracellular Mg^{2+} has two opposing effects on the activation of the mslo1 channel: activating the channel by binding to the low affinity Mg^{2+}/Ca^{2+} sites, and inhibiting Ca^{2+}-dependent activation by competitively binding to the high affinity Ca^{2+} sites. Neither effect of Mg^{2+} changes the dissociation constants of Ca^{2+} binding to the channel at the open or closed conformation. In other words, Mg^{2+} does not affect the intrinsic Ca^{2+} affinity for the channel or the efficacy of Ca^{2+} in activating the channel. However, the combination of these two effects of Mg^{2+} changes the Ca^{2+} dose-response of channel activation as shown in Fig. 6. The $[Ca^{2+}]_i$ dependence of the steady-state open probability (G/G_{max}) at 0 (Fig. 6 C) or 10 mM $[Mg^{2+}]_i$ (Fig. 6 D) are shown with voltages at −40–100 mV and −80–60 mV, respectively. Since at low $[Ca^{2+}]_i$ both the activation and inhibition effects of Mg^{2+} are manifested, whereas at high $[Ca^{2+}]_i$ the inhibition effect is diminished, the curve in the presence of 10 mM $[Mg^{2+}]_i$ is more sigmoidal than that in the absence of Mg^{2+} at a certain voltage. This difference is reflected in Fig. 6 E where the Hill coefficient in the presence of 10 mM $[Mg^{2+}]_i$ is larger than that in the absence of Mg^{2+} at all voltages. Fig. 6 F shows that at all voltages the apparent K_d from Hill fits is smaller in the presence of 10 mM $[Mg^{2+}]_i$. These results demonstrate that the effect of Mg^{2+} on the channel activation is to increase the apparent Ca^{2+} sensitivity of channel activation.

DISCUSSION

We have investigated three effects of intracellular Mg^{2+} on the mslo1 BK type Ca^{2+}-activated K^+ channel: (1) the block of the channel pore, (2) the allosteric activation of the channel, and (3) the competitive inhibition of Ca^{2+}-dependent activation. Our results suggest that these effects are underlined by three distinct classes of Mg^{2+} binding sites and separate molecular mechanisms. Mg^{2+} binds to a site that may be in the inner mouth of the pore with rapid binding/unbinding kinetics and blocks the ion permeation. By binding to a class of low affinity Mg^{2+}/Ca^{2+} sites Mg^{2+} activates the channel. Mg^{2+} also binds to the high affinity Ca^{2+} sites and inhibits Ca^{2+}-dependent activation by preventing Ca^{2+} from binding to the same site.

Previous studies have shown that intracellular Mg^{2+} blocks BK channels and changes channel activation. Single-channel studies have revealed that the voltage-dependent block of Mg^{2+} ($K_d \sim 30$ mM at 0 mV) results in a reduced single-channel conductance at positive voltages due to the rapid binding kinetics (Ferguson, 1991; Laver, 1992; Morales et al., 1996; Wachter and Turnheim, 1996). Our results from the study of macroscopic currents are consistent with this mechanism. The mechanisms of Mg^{2+} effects on channel activation, on the other hand, were not clear. Golowasch et al. (1986) discovered that intracellular Mg^{2+} (at concentrations 1–10 mM) changed the Ca^{2+} dependence of BK channel open probabilities, increasing the Hill coefficient from 2 to as high as 5.8. Under their experimental conditions, Mg^{2+} did not activate the channel in the absence of Ca^{2+}. These results led to their conclusion that Mg^{2+}, as a modulator of Ca^{2+}-dependent activation, revealed Ca^{2+} sites already present in the channel protein in the absence of Mg^{2+}. By studying the effects of divalent cations Oberhauser et al. (1988) further supported this mechanism. Other subsequent studies also found similar results that Mg^{2+} was unable to open the channel by itself and its effect on channel activation was dependent on $[Ca^{2+}]_i$ (Squire and Petersen, 1987; Trieschmann and Isenberg, 1989; Zamoyski et al., 1989; McLarnon and Sawyer, 1993; Zhang et al., 1995; Bringmann et al., 1997). However, the

mechanism proposed by Golowasch et al. (1986) cannot account for the observation that the open probability of some BK channels increased at high $[Ca^{2+}]_i$ but decreased at low $[Ca^{2+}]_i$ ($\leq$10 μM) after adding Mg^{2+} (at concentrations 2–5 mM; Komatsu et al., 1996; Kazachenko and Chemeris, 1998). A recent study of the mslo1 homologue from *Drosophila*, dslo, suggested that dslo might contain as many as eight Ca^{2+} binding sites since the Hill coefficient of the channel's response to $[Ca^{2+}]_i$ was larger than four. Nevertheless, such a high Hill coefficient was obtained in the absence of intracellular Mg^{2+}, which did not address the role of Mg^{2+} in the function of Ca^{2+}-dependent activation (Bian et al., 2001). In the studies presented here, we recorded macroscopic currents that enabled us to observe the channel activation at much wider range of voltages than previous single-channel studies. Our results demonstrate that Mg^{2+} activates BK channels independently of Ca^{2+}. On the other hand, Mg^{2+} may competitively inhibit Ca^{2+}-dependent activation. Neither effect changes the intrinsic Ca^{2+} affinity for its binding site or the efficacy of Ca^{2+} in activating the channel upon binding. However, these two opposing effects result in the change of the Ca^{2+} dose-response of channel activation and an enhanced Hill coefficient. It is important to note that the Hill coefficient in our results is no larger than four, even in the presence of 10 mM $[Mg^{2+}]_i$ (Fig. 6 E), which is consistent with our conclusion that no additional high affinity Ca^{2+} sites in the mslo1 channel are exposed by Mg^{2+}. This result is qualitatively different from the result of Golowasch et al. (1986) and the reason for such discrepancy needs to be further investigated.

Three Distinct Classes of Binding Sites for Intracellular Divalent Cations

The sites for Mg^{2+}-dependent activation are distinct from the site for Mg^{2+} block in mslo1 channels. Three lines of evidence lead to this conclusion: first, Mg^{2+}-dependent activation has different voltage dependence from Mg^{2+} block (Fig. 1). Second, Mg^{2+} that blocks the BK channel binds to a site in the channel pore with a bimolecular interaction (Fig. 1; Ferguson, 1991; Laver, 1992). On the other hand, there are at least two cooperative binding sites for Mg^{2+} in the activation of a mslo1 channel (Figs. 2 and 4). Third, Mg^{2+} does not activate the mslo3 channel, but blocks it similarly as to mslo1 (Fig. 3 B). This conclusion is also consistent with previous results that the potency of various cations in blocking BK channels follows a different sequence than the effectiveness of divalent cations in activating the channel (Oberhauser et al., 1988). Different voltage dependence of Mg^{2+}-dependent activation and Mg^{2+} block was also observed in smooth muscle BK channels (Zhang et al., 1995).

The sites for Mg^{2+}-dependent activation do not seem to discriminate between Mg^{2+} and Ca^{2+} as far as the effect on channel activation is concerned (Figs. 1 B and 5 B; see Zhang et al., 2001, in this issue). Mg^{2+} (or Ca^{2+}) activates the channel because the affinity of these sites is higher at the open conformations than at the closed. It is interesting that both Mg^{2+} and Ca^{2+} activate the channel with similar effectiveness through the low affinity sites although the ionic radius of Mg^{2+} (0.7 Å) differs from Ca^{2+} (1.2 Å) quite significantly. It suggests that these sites may not be sensitive to the size of divalent cations at either open or closed conformations. On the contrary, the effectiveness of divalent cations in activating the channel through the high affinity Ca^{2+} sites seems to be based on their radii. Only cations with radii $>$0.72 Å (Co^{2+}) or $<$1.13 Å (Sr^{2+}) are able to activate the channel and the effectiveness increases with larger radii within this range (Oberhauser et al., 1988). Consistent with the findings by Oberhauser et al. (1988), our results show that Mg^{2+} is too small to activate the mslo1 channel through the high affinity Ca^{2+} sites. However, we find that Mg^{2+} can bind to these sites and effectively compete with Ca^{2+} although the affinity of Mg^{2+} for these sites is much lower. These results suggest that the conformational change at these sites during channel activation may be just large enough to affect the affinity for large cations with radii $>$0.72 Å (Co^{2+}) but not enough for small cations like Mg^{2+}.

Extracellular Mg^{2+} has been shown to screen negative charges on the external surface of BK channels, resulting in a shift of the voltage activation curve (MacKinnon et al., 1989). This screen effect was nonselective among cations because external Na^+ and K^+ also resulted in similar shifts of the voltage activation curve (MacKinnon et al., 1989). This shift could be well fitted with the Gouy-Chapman model that quantitatively describes the effects of surface potential on the activation of various ion channels (Hille et al., 1975; McLaughlin, 1977; MacKinnon et al., 1989). Unlike these results with external cations, the $[Mg^{2+}]_i$ dependence of the G-V shift is much steeper than the $[Mg^{2+}]_o$-dependent shifts, with about −50 mV change of $\Delta V_{1/2}$ between $[Mg^{2+}]_i$ of 1 and 10 mM (Fig. 2 C). Such a steep $[Mg^{2+}]_i$ dependence cannot be accounted for by the screen effect because the Gouy-Chapman model has a maximum possible slope of only 29.3 mV per 10- fold change in $[Mg^{2+}]_i$ at our experimental temperature (Hille et al., 1975).

The Allosteric Linkage among Mg^{2+}, Ca^{2+}, and Voltage-dependent Activation

Previous results have demonstrated that Ca^{2+} and voltage do not directly interact in activating the mslo1 channel, but are energetically linked through the transition between closed and open conformations of the

channel (Cui and Aldrich, 2000). The results in Fig. 2 D further support this conclusion because Ca^{2+} binding at 110 μM $[Ca^{2+}]_i$ contributes the same energy of 23 kcal/mol to channel activation at 0 or 10 mM $[Mg^{2+}]_i$, although the voltage range of channel activation is 65 mV apart. Similarly, Mg^{2+}-dependent activation of the mslo1 channel derives from the difference of its affinity for the channel at open or closed conformations (Fig. 4). It does not directly depend on Ca^{2+} or voltage (Figs. 1 and 2), but it is influenced by voltage and Ca^{2+} because they affect conformational changes during channel activation. It is striking that three separate pathways affect the transition between closed and open conformations of the mslo1 channel with a similar allosteric mechanism (Cox et al., 1997a; Horrigan et al., 1999; Cui and Aldrich, 2000):

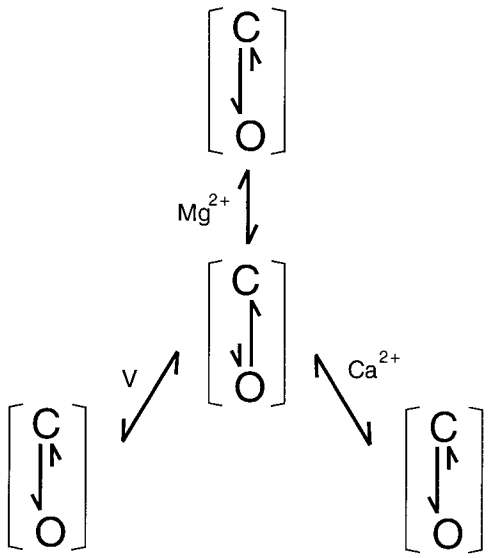

(SCHEME III)

Mg^{2+}, Ca^{2+}, and depolarization all shift the C-O transition towards open conformations and promote the activation of the channel. However, they do not directly interact with each other during activation. In this study, we found that Mg^{2+} activated the mslo1 channel by shifting the G-V relation to more negative voltage ranges. The G-V relation at all $[Mg^{2+}]_i$ could be well fitted with the Boltzmann equation with a similar slope (Fig. 2, A and B). These characteristics are similar to those of Ca^{2+}-dependent activation (Fig. 6; Cui et al., 1997). Therefore, the voltage dependence of the channel in Schemes I II is simplified as a one-step transition between open and closed conformations (Cox et al., 1997a; Horrigan et al., 1999; Cui and Aldrich, 2000).

The pathways of channel activation start with the voltage sensor and ionic binding sites. Similar to other voltage-dependent channels, the S4 transmembrane segment is likely to be part of the voltage sensor in mslo1 channels (Yang and Horn, 1995; Aggarwal and MacKinnon, 1996; Mannuzzu et al., 1996; Seoh et al., 1996;

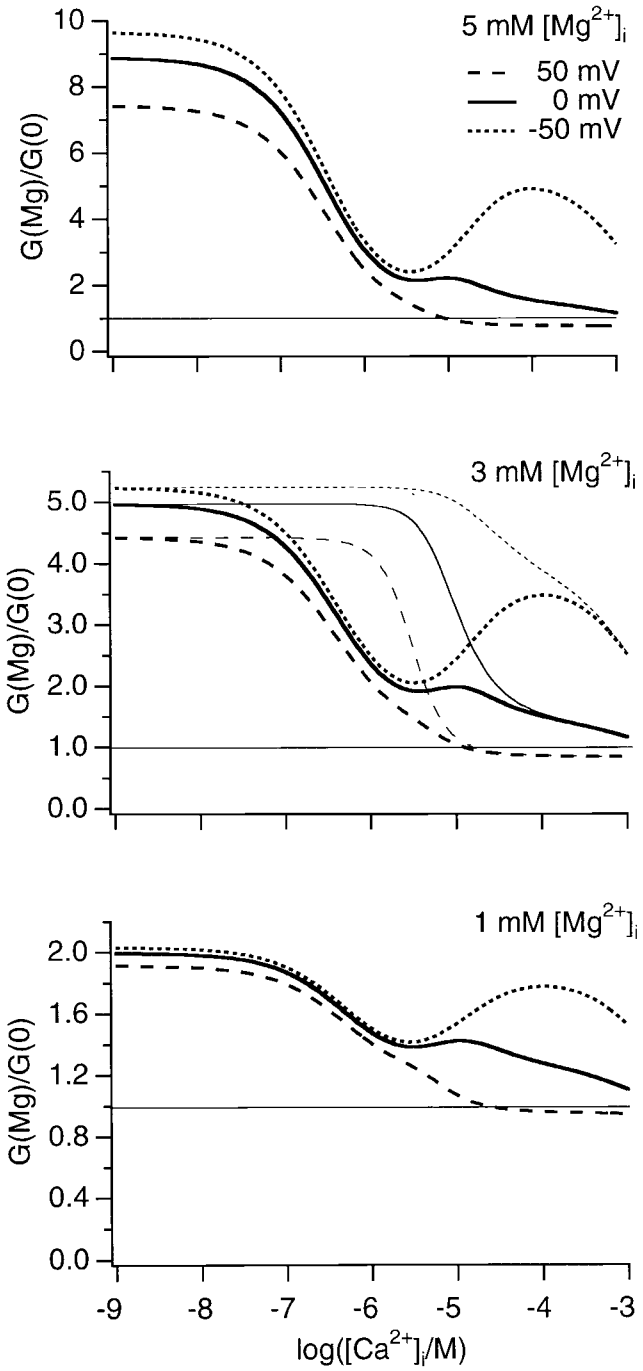

FIGURE 7. The ratio of conductance with or without intracellular Mg^{2+}. The conductance, $G = \gamma P_o$, in the presence of 5, 3, or 1 mM $[Mg^{2+}]_i$ versus that in the absence of Mg^{2+} are plotted against $[Ca^{2+}]_i$ (top to bottom), where γ is the single-channel conductance. Results at three physiological voltages (50, 0, and −50 mV) are displayed. The horizontal straight line indicates the ratio of 1. P_o is computed from Eq. 2∼5 with parameters described in Fig. 2 legends and Scheme II footnote. γ is computed from the Woodhull model and the parameters described in Fig. 1 legend. We assume that Ca^{2+} is equivalent to Mg^{2+} in blocking the channel (Cox et al., 1997b) and in activating the channel by binding to the low affinity Mg^{2+}/Ca^{2+} sites (Fig. 5). Therefore, even in the absence of Mg^{2+}, the low affinity Mg^{2+}/Ca^{2+} sites are occupied by Ca^{2+} and contribute to activation; similarly, the channel is blocked by Ca^{2+}. At 3 mM $[Mg^{2+}]_i$ (middle) we also computed the ratio of conductance without considering the competition of Mg^{2+} at the high affinity Ca^{2+} sites (thin curves).

Yang et al., 1996; Diaz et al., 1998; Cui and Aldrich, 2000). The high affinity Ca^{2+} sites are located in the tail domain of mslo1 subunits, including the Ca^{2+} bowl that contains repeated aspartate and glutamate residues (Moss et al., 1996; Schreiber and Salkoff, 1997; Schreiber et al., 1999; Bian et al., 2001). The structural identity of the low affinity Mg^{2+}/Ca^{2+} sites is not clear, but our results indicate that they are located in the core domain (Fig. 3). Recently, the X-ray crystal structure of the RCK domain (a structural domain for regulating the conductance of K^+ channels) of the *E. coli* K^+ channel has been solved (Jiang et al., 2001). The core of the RCK domain forms a Rossmann fold that usually contains a binding site for a metal ion. The core of slo channels also contains a RCK domain (Fig. 3, A and D) with a similar structure (Jiang et al., 2001). Therefore, it is likely that the low affinity Mg^{2+}/Ca^{2+} site resides in the RCK domain. The primary sequence of the RCK domain in slo channels is flanked by the S6 transmembrane domain, which may be part of the activation gate (Yellen, 1998), on one side and the tail domain that contains the Ca^{2+} bowl (Schreiber et al., 1999) on the other. This position and other mutation experiments suggest the RCK to be important in the function of BK channels, possibly involved in Ca^{2+} and voltage-dependent gating (Jiang et al., 2001). The prospect that the low affinity Mg^{2+}/Ca^{2+} site is also located in the RCK domain is intriguing because it suggests that all three pathways that activate the BK channel might converge at the RCK domain.

Intracellular Mg^{2+} Enhances BK Channel Function at Physiological Conditions

The three effects of Mg^{2+} on mslo1 channels are opposite in changing the K^+ current across membrane, each with a specific dependence on voltage, $[Ca^{2+}]_i$, and $[Mg^{2+}]_i$. Therefore, their contribution to cell physiology is complex. By combining the quantitative description of all three individual effects we are able to simulate the overall effect of Mg^{2+} on the whole cell BK channel conductance (Fig. 7). It is clear that, at voltages below 0 mV, $[Mg^{2+}]_i$ of ~1–5 mM enhances BK channel function over the entire range of $[Ca^{2+}]_i$. Even at $[Ca^{2+}]_i$ of ~10–100 μM, where the channel has a substantial open probability (≥0.1; Fig. 6), BK channel conductance is increased by ~30–100%. Such an increase enhances the polarization of membrane potential by BK channels and can lead to significant consequences in neurotransmitter release, electric tuning in cochlear hair cells, and smooth muscle contraction. In these physiological processes, BK channels are co-localized with voltage-dependent Ca^{2+} channels (Roberts et al., 1990; Robitaille et al., 1993; Yazejian et al., 1997; Marrion and Tavalin, 1998; Yazejian et al., 2000) or RYR (Jaggar et al., 2000) and functionally coupled to them by sensing the Ca^{2+} entering cytosol through these channels. Due to the spacial proximity between BK channels and voltage-dependent Ca^{2+} channels or ryanodine receptors the local $[Ca^{2+}]_i$ surrounding these BK channels is >10 μM (Roberts, 1994; Neher, 1998; Jaggar et al., 2000; Yazejian et al., 2000).

The contribution of each Mg^{2+} effect on BK channel conductance is particularly prominent at specific voltage and $[Ca^{2+}]_i$ ranges. For example, since the open probability of mslo1 channels is close to 1 at 50 mV and $[Ca^{2+}]_i \geq 10$ μM Mg^{2+} can no longer increase it. The only observable effect of Mg^{2+} is to block the channel. Therefore, the whole cell BK channel conductance is reduced by Mg^{2+} under this condition (Fig. 7). The combined Mg^{2+} block and Mg^{2+}-dependent activation, but not the competitive inhibition of Ca^{2+}-dependent activation, is also plotted in Fig. 7 at 3 mM $[Mg^{2+}]_i$ (middle, thin curves). The comparison of this result with the ones that include the competitive inhibition (Fig. 7, thick curves) demonstrates that the competitive inhibition of Ca^{2+}-dependent activation by Mg^{2+} results in a significant reduction of the Mg^{2+}-dependent activation at $[Ca^{2+}]_i$ of ~0.1–100 μM.

The mslo1, mslo3, and mslo3 tail clones were provided to us by Larry Salkoff. The mslo1 core clone was provided to us by Yasushi Okamura. We thank Victor Corvalan for algorithms for Ca^{2+} concentration calculations, Karl Magleby for helpful discussion on issues related to surface charges, Gayathri Krishnamoorthy, Stephen W. Jones, and Rick Aldrich for comments on the manuscript.

This work was supported by a Scientist Development Grant from the American Heart Association (9930025N to J. Cui).

Submitted: 3 July 2001
Revised: 28 August 2001
Accepted: 17 September 2001

REFERENCES

Adelman, J.P., K.Z. Shen, M.P. Kavanaugh, R.A. Warren, Y.N. Wu, A. Lagrutta, C.T. Bond, and R.A. North. 1992. Calcium-activated potassium channels expressed from cloned complementary DNAs. *Neuron.* 9:209–216.

Aggarwal, S.K., and R. MacKinnon. 1996. Contribution of the S4 segment to gating charge in the *Shaker* K^+ channel. *Neuron.* 16: 1169–1177.

Altura, B.M., B.T. Altura, A. Carella, A. Gebrewold, T. Murakawa, and A. Nishio. 1987. Mg^{2+}-Ca^{2+} interaction in contractility of vascular smooth muscle: Mg^{2+} versus organic calcium channel blockers on myogenic tone and agonist- induced responsiveness of blood vessels. *Can. J. Physiol. Pharmacol.* 65:729–745.

Altura, B.M., and R.K. Gupta. 1992. Cocaine induces intracellular free Mg deficits, ischemia and stroke as observed by in-vivo 31P-NMR of the brain. *Biochim. Biophys. Acta.* 1111:271–274.

Atkinson, N.S., G.A. Robertson, and B. Ganetzky. 1991. A component of calcium-activated potassium channels encoded by the *Drosophila* slo locus. *Science.* 253:551–555.

Bian, S., I. Favre, and E. Moczydlowski. 2001. Ca^{2+}-binding activity of a COOH-terminal fragment of the *Drosophila* BK channel involved in Ca^{2+}-dependent activation. *Proc. Natl. Acad. Sci. USA.* 98:4776–4781.

Brenner, R., G.J. Perez, A.D. Bonev, D.M. Eckman, J.C. Kosek, S.W. Wiler, A.J. Patterson, M.T. Nelson, and R.W. Aldrich. 2000. Vasoregulation by the beta1 subunit of the calcium-activated potassium channel. *Nature.* 407:870–876.

Bringmann, A., F. Faude, and A. Reichenbach. 1997. Mammalian

retinal glial (Muller) cells express large-conductance Ca^{2+}-activated K^+ channels that are modulated by Mg^{2+} and pH and activated by protein kinase A. *Glia.* 19:311–323.

Butler, A., S. Tsunoda, D.P. McCobb, A. Wei, and L. Salkoff. 1993. mSlo, a complex mouse gene encoding "maxi" calcium-activated potassium channels. *Science.* 261:221–224.

Chuang, H., Y.N. Jan, and L.Y. Jan. 1997. Regulation of IRK3 inward rectifier K^+ channel by m1 acetylcholine receptor and intracellular magnesium. *Cell.* 89:1121–1132.

Colquhoun, D. 1998. Binding, gating, affinity and efficacy: the interpretation of structure- activity relationships for agonists and of the effects of mutating receptors. *Br. J. Pharmacol.* 125:924–947.

Corkey, B.E., J. Duszynski, T.L. Rich, B. Matschinsky, and J.R. Williamson. 1986. Regulation of free and bound magnesium in rat hepatocytes and isolated mitochondria. *J. Biol. Chem.* 261:2567–2574.

Cox, D.H., J. Cui, and R.W. Aldrich. 1997a. Allosteric gating of a large conductance Ca-activated K^+ channel. *J. Gen. Physiol.* 110: 257–281.

Cox, D.H., J. Cui, and R.W. Aldrich. 1997b. Separation of gating properties from permeation and block in mslo large conductance Ca-activated K^+ channels. *J. Gen. Physiol.* 109:633–646.

Cui, J., and R.W. Aldrich. 2000. Allosteric linkage between voltage and Ca^{2+}-dependent activation of BK-type mslo1 $K(^+)$ channels. *Biochemistry.* 39:15612–15619.

Cui, J., D.H. Cox, and R.W. Aldrich. 1997. Intrinsic voltage dependence and Ca^{2+} regulation of mslo large conductance Ca-activated K^+ channels. *J. Gen. Physiol.* 109:647–673.

Diaz, L., P. Meera, J. Amigo, E. Stefani, O. Alvarez, L. Toro, and R. Latorre. 1998. Role of the S4 segment in a voltage-dependent calcium-sensitive potassium (hSlo). *J Biol Chem.* 273:32430–32436.

Fabiato, A., and F. Fabiato. 1979. Calculator programs for computing the composition of the solutions containing multiple metals and ligands used for experiments in skinned muscle cells. *J Physiol.* 75:463–505.

Ferguson, W.B. 1991. Competitive Mg^{2+} block of a large-conductance, Ca^{2+}-activated K^+ channel in rat skeletal muscle. Ca^{2+}, Sr^{2+}, and Ni^{2+} also block. *J. Gen. Physiol.* 98:163–181.

Flatman, P.W. 1984. Magnesium transport across cell membranes. *J Membr. Biol.* 80:1–14.

Flatman, P.W. 1991. Mechanisms of magnesium transport. *Annu Rev Physiol.* 53:259–271.

Golowasch, J., A. Kirkwood, and C. Miller. 1986. Allosteric effects of Mg^{2+} on the gating of Ca^{2+}-activated K^+ channels from mammalian skeletal muscle. *J. Exp. Biol.* 124:5–13.

Gupta, R.K., P. Gupta, and R.D. Moore. 1984. NMR studies of intracellular metal ions in intact cells and tissues. *Annu. Rev. Biophys. Bioeng.* 13:221–246.

Hille, B., A.M. Woodhull, and B.I. Shapiro. 1975. Negative surface charge near sodium channels of nerve: divalent ions, monovalent ions, and pH. *Philos. Trans. R. Soc. Lond. B Biol. Sci.* 270:301–318.

Horrigan, F.T., and R.W. Aldrich. 1999. Allosteric voltage gating of potassium channels II. Mslo channel gating charge movement in the absence of Ca^{2+}. *J. Gen. Physiol.* 114:305–336.

Horrigan, F.T., J. Cui, and R.W. Aldrich. 1999. Allosteric voltage gating of potassium channels I. Mslo ionic currents in the absence of Ca^{2+}. *J. Gen. Physiol.* 114:277–304.

Hudspeth, A.J., and R.S. Lewis. 1988a. Kinetic analysis of voltage- and ion-dependent conductances in saccular hair cells of the bull-frog, Rana catesbeiana. *J. Physiol.* 400:237–274.

Hudspeth, A.J., and R.S. Lewis. 1988b. A model for electrical resonance and frequency tuning in saccular hair cells of the bull-frog, Rana catesbeiana. *J. Physiol.* 400:275–297.

Jaggar, J.H., V.A. Porter, W.J. Lederer, and M.T. Nelson. 2000. Calcium sparks in smooth muscle. *Am. J. Physiol. Cell Physiol.* 278: C235–C256.

Jiang, Y., A. Pico, M. Cadene, B.T. Chait, and R. MacKinnon. 2001. Structure of the RCK domain from the E. coli K^+ channel and demonstration of its presence in the human BK channel. *Neuron.* 29:593–601.

Kazachenko, V.N., and N.K. Chemeris. 1998. Modulation of the activity of Ca^{2+}-activated K^+ channels by internal Mg^{2+} in cultured kidney cells vero. *Membr. Cell Biol.* 12:489–511.

Komatsu, H., H. Mieno, K. Tamaki, M. Inoue, G. Kajiyama, and I. Seyama. 1996. Modulation of Ca^{2+}-activated K^+ channels by Mg^{2+} and ATP in frog oxyntic cells. *Pflügers Arch.* 431:494–503.

Laurant, P., and R.M. Touyz. 2000. Physiological and pathophysiological role of magnesium in the cardiovascular system: implications in hypertension. *J. Hypertens.* 18:1177–1191.

Laver, D.R. 1992. Divalent cation block and competition between divalent and monovalent cations in the large-conductance K^+ channel from *Chara australis*. *J. Gen. Physiol.* 100:269–300.

MacKinnon, R., R. Latorre, and C. Miller. 1989. Role of surface electrostatics in the operation of a high-conductance Ca^{2+}-activated K^+ channel. *Biochemistry.* 28:8092–8099.

Mannuzzu, L.M., M.M. Moronne, and E.Y. Isacoff. 1996. Direct physical measure of conformational rearrangement underlying potassium channel gating. *Science.* 271:213–216.

Marrion, N.V., and S.J. Tavalin. 1998. Selective activation of Ca^{2+}-activated K^+ channels by co-localized Ca^{2+} channels in hippocampal neurons. *Nature.* 395:900–905.

Marty, A. 1981. Ca-dependent K channels with large unitary conductance in chromaffin cell membranes. *Nature.* 291:497–500.

Matsuda, H., A. Saigusa, and H. Irisawa. 1987. Ohmic conductance through the inwardly rectifying K channel and blocking by internal Mg^{2+}. *Nature.* 325:156–159.

McLarnon, J.G., and D. Sawyer. 1993. Effects of divalent cations on the activation of a calcium-dependent potassium channel in hippocampal neurons. *Pflugers Arch.* 424:1–8.

McLaughlin, S. 1977. Electrostatic potentials at membrane-solution interfaces. *Curr. Top. Membr. Transp.* 9:71–144.

McManus, O.B., and K.L. Magleby. 1991. Accounting for the Ca^{2+}-dependent kinetics of single large- conductance Ca^{2+}-activated K^+ channels in rat skeletal muscle. *J. Physiol.* 443:739–777.

Meera, P., M. Wallner, Z. Jiang, and L. Toro. 1996. A calcium switch for the functional coupling between alpha (hslo) and beta subunits (KV,Ca beta) of maxi K channels. *FEBS Lett.* 382:84–88.

Monod, J., J. Wyman, and J.P. Changeux. 1965. On the nature of allosteric transitions: a plausible model. *J. Mol. Biol.* 12:88–118.

Morales, E., W.C. Cole, C.V. Remillard, and N. Leblane. 1996. Block of large conductance Ca^{2+}-activated K^+ channels in rabbit vascular myocytes by internal Mg^{2+} and Na^+. *J. Physiol.* 495:701–716.

Moss, G.W., J. Marshall, and E. Moczydlowski. 1996. Hypothesis for a serine proteinase-like domain at the COOH terminus of Slowpoke calcium-activated potassium channels. *J. Gen. Physiol.* 108:473–484.

Neher, E. 1998. Vesicle pools and Ca^{2+} microdomains: new tools for understanding their roles in neurotransmitter release. *Neuron.* 20:389–399.

Nelson, M.T., H. Cheng, M. Rubart, L.F. Santana, A.D. Bonev, H.J. Knot, and W.J. Lederer. 1995. Relaxation of arterial smooth muscle by calcium sparks. *Science.* 270:633–637.

Oberhauser, A., O. Alvarez, and R. Latorre. 1988. Activation by divalent cations of a Ca^{2+}-activated K^+ channel from skeletal muscle membrane. *J. Gen. Physiol.* 92:67–86.

Pallotta, B.S. 1985. N-bromoacetamide removes a calcium-dependent component of channel opening from calcium-activated potassium channels in rat skeletal muscle. *J. Gen. Physiol.* 86:601–611.

Pallotta, B.S., K.L. Magleby, and J.N. Barrett. 1981. Single channel recordings of Ca^{2+}-activated K^+ currents in rat muscle cell culture. *Nature.* 293:471–474.

Pluger, S., J. Faulhaber, M. Furstenau, M. Lohn, R. Waldschutz, M.

Gollasch, H. Haller, F.C. Luft, H. Ehmke, and O. Pongs. 2000. Mice with disrupted BK channel beta1 subunit gene feature abnormal Ca^{2+} spark/STOC coupling and elevated blood pressure. *Circ. Res.* 87:E53–E60.

Roberts, W.M. 1994. Localization of calcium signals by a mobile calcium buffer in frog saccular hair cells. *J. Neurosci.* 14:3246–3262.

Roberts, W.M., R.A. Jacobs, and A.J. Hudspeth. 1990. Colocalization of ion channels involved in frequency selectivity and synaptic transmission at presynaptic active zones of hair cells. *J. Neurosci.* 10:3664–3684.

Robitaille, R., M.L. Garcia, G.J. Kaczorowski, and M.P. Charlton. 1993. Functional colocalization of calcium and calcium-gated potassium channels in control of transmitter release. *Neuron.* 11: 645–655.

Romani, A.M., V.D. Matthews, and A. Scarpa. 2000. Parallel stimulation of glucose and Mg^{2+} accumulation by insulin in rat hearts and cardiac ventricular myocytes. *Circ. Res.* 86:326–333.

Schreiber, M., and L. Salkoff. 1997. A novel calcium-sensing domain in the BK channel. *Biophys. J.* 73:1355–1363.

Schreiber, M., A. Wei, A. Yuan, J. Gaut, M. Saito, and L. Salkoff. 1998. Slo3, a novel pH-sensitive K^+ channel from mammalian spermatocytes. *J. Biol. Chem.* 273:3509–3516.

Schreiber, M., A. Yuan, and L. Salkoff. 1999. Transplantable sites confer calcium sensitivity to BK channels. *Nat. Neurosci.* 2:416–421.

Seelig, M.S. 2000. Interrelationship of magnesium and congestive heart failure. *Wien Med. Wochenschr.* 150:335–341.

Seoh, S.A., D. Sigg, D.M. Papazian, and F. Bezanilla. 1996. Voltage-sensing residues in the S2 and S4 segments of the Shaker K^+ channel. *Neuron.* 16:1159–1167.

Shen, K.Z., A. Lagrutta, N.W. Davies, N.B. Standen, J.P. Adelman, and R.A. North. 1994. Tetraethylammonium block of Slowpoke calcium-activated potassium channels expressed in *Xenopus* oocytes: evidence for tetrameric channel formation. *Pflügers Arch.* 426:440–445.

Squire, L.G., and O.H. Petersen. 1987. Modulation of Ca^{2+}- and voltage-activated K^+ channels by internal Mg^{2+} in salivary acinar cells. *Biochim. Biophys. Acta.* 899:171–175.

Stryer, L. 1995. Biochemistry. W. H. Freeman and Company, New York. 1064 pp.

Trieschmann, U., and G. Isenberg. 1989. Ca^{2+}-activated K^+ channels contribute to the resting potential of vascular myocytes. Ca^{2+}-sensitivity is increased by intracellular Mg^{2+}- ions. *Pflügers Arch.* 414:S183–S184.

Vandenberg, C.A. 1987. Inward rectification of a potassium channel in cardiac ventricular cells depends on internal magnesium ions. *Proc. Natl. Acad. Sci. USA.* 84:2560–2564.

Vink, R., and I. Cernak. 2000. Regulation of intracellular free magnesium in central nervous system injury. *Front Biosci.* 5:D656–D665.

Wachter, C., and K. Turnheim. 1996. Inhibition of high-conductance, calcium-activated potassium channels of rabbit colon epithelium by magnesium. *J. Membr. Biol.* 150:275–282.

Wei, A., C. Solaro, C. Lingle, and L. Salkoff. 1994. Calcium sensitivity of BK-type KCa channels determined by a separable domain. *Neuron.* 13:671–681.

White, R.E., and H.C. Hartzell. 1988. Effects of intracellular free magnesium on calcium current in isolated cardiac myocytes. *Science.* 239:778–780.

Woodhull, A.M. 1973. Ionic blockage of sodium channels in nerve. *J. Gen. Physiol.* 61:687–708.

Wu, Y.C., J.J. Art, M.B. Goodman, and R. Fettiplace. 1995. A kinetic description of the calcium-activated potassium channel and its application to electrical tuning of hair cells. *Prog. Biophys. Mol. Biol.* 63:131–158.

Yang, N., A.J. George, and R. Horn. 1996. Molecular basis of charge movement in voltage-gated sodium channels. *Neuron.* 16:113–122.

Yang, N., and R. Horn. 1995. Evidence for voltage-dependent S4 movement in sodium channels. *Neuron.* 15:213–218.

Yazejian, B., D.A. DiGregorio, J.L. Vergara, R.E. Poage, S.D. Meriney, and A.D. Grinnell. 1997. Direct measurements of presynaptic calcium and calcium-activated potassium currents regulating neurotransmitter release at cultured Xenopus nerve-muscle synapses. *J. Neurosci.* 17:2990–3001.

Yazejian, B., X.P. Sun, and A.D. Grinnell. 2000. Tracking presynaptic Ca^{2+} dynamics during neurotransmitter release with Ca^{2+}-activated K^+ channels. *Nat. Neurosci.* 3:566–571.

Yellen, G. 1998. The moving parts of voltage-gated ion channels. *Q. Rev. Biophys.* 31:239–295.

Zagotta, W.N. 2001. Structure that opens the gate and opens the door. *Neuron.* 29:547–548.

Zamoyski, V.L., V.N. Serebryakov, and R. Schubert. 1989. Activation and blocking effects of divalent cations on the calcium-dependent potassium channel of high conductance. *Biomed. Biochim. Acta.* 48:S388–S392.

Zhang, X., E. Puil, and D.A. Mathers. 1995. Effects of intracellular Mg^{2+} on the properties of large-conductance, Ca^{2+}-dependent K^+ channels in rat cerebrovascular smooth muscle cells. *J. Cereb. Blood Flow Metab.* 15:1066–1074.

Zhang, X., C.R. Solaro, and C.J. Lingle. 2001. Allosteric regulation of BK channel gating by Ca^{2+} and Mg^{2+} through a nonselective low affinity divalent cation site. *J. Gen. Physiol.* 118:607–635.